

# Robust Low-rank Tensor Regression via Clipping and Huber Loss

Kangqiang Li<sup>a,b</sup>, Bingqi Liu<sup>b,\*</sup>, Yang Yang<sup>a</sup>, Li Wang<sup>c</sup>

<sup>a</sup>*Information Center, Hubei Provincial Tobacco Monopoly  
Administration, Wuhan 430030, Hubei, China*

<sup>b</sup>*School of Mathematical Sciences, Zhejiang  
University, Hangzhou 310058, Zhejiang, China*

<sup>c</sup>*Procurement Management Office, Hubei Provincial Tobacco Monopoly  
Administration, Wuhan 430030, Hubei, China*

---

## Abstract

In this paper, we construct a parameter estimation framework for robust low-rank tensor regression based on a truncation method and Huber loss, specifically focusing on models with random noise having only finite second-order moments. Through a robust gradient descent method, our proposed Huber-type estimator is theoretically optimal in two aspects: (1) its statistical error rate matches the optimal upper bound established for the traditional least squares method under sub-Gaussian error; and (2) the sample complexity for recovering the tensor parameter is also optimal. Extensive numerical experiments demonstrate the robustness of our estimator, indicating that the utilization of truncation and Huber loss significantly enhances stability and statistical effectiveness, outperforming the traditional least squares method. Additionally, the phenomenon of phase transition in the convergence rate of

---

\*Corresponding author

*Email addresses:* 11935023@zju.edu.cn (Kangqiang Li), bqliu@zju.edu.cn (Bingqi Liu)

the proposed estimator is confirmed through simulation. Furthermore, applications to image recovery and the Beijing air-quality dataset demonstrate the practical effectiveness of our method.

*Keywords:* Tensor regression, Huber loss, Truncation, Heavy tails, Robust estimation

*2020 MSC:* 62F35, 62H12, 68T05, 15A69

---

## 1. Introduction

In recent years, the tail-robustness issue in parameter regression estimation has become an interesting research highlight. A primary reason for this attention is that many well-used statistical methods and algorithms based on the sub-Gaussian assumption suffer from heavy-tailed distribution and the real-world datasets, especially in the financial area, often exhibit heavy tails. Therefore, some effective approaches to adequately estimate regression parameter with the heavy-tailed noise have been proposed by numerous literature. One of the popular ways is to replace the traditional squared loss with robust alternatives such as absolute loss, quantile loss, Huber loss (Huber, 1964) and Cauchy loss. This type of robust technique was originally aimed at achieving the outlier-robustness. Recently, Fan et al. (2016) first employed the Huber loss into linear regression problem to investigate the robustness against heavy-tailness of the regression error. Their theoretical result unveils that under only finite second order moment condition on the noise, the proposed robust estimator has the same optimal rate as the case of sub-Gaussian tails via carefully tuning the robustification parameter of Huber loss. Sun et al. (2020) revisited this adaptive Huber regression with

only bounded  $(1 + \epsilon)$ -th moment noise, and found a tight phase transition phenomenon for the convergence rate of the regression parameter. [Wang et al. \(2021\)](#) proposed a data-driven approach for Huber-type robust mean estimation and linear regression such that the robustification parameter can efficiently be tuned. There are also a broad range of other literature using the adaptive Huber loss to study regression problems with heavy-tailed errors (see, for example, [Zhou et al. \(2018\)](#) and [Luo and Gao \(2022\)](#) for linear regression, [Fan et al. \(2019\)](#) for large-scale multiple testing, [Shen et al. \(2025\)](#) for matrix recovery and [Fan et al. \(2024\)](#) for neural networks).

Another convenient and effective way to handle heavy-tailed data is to directly clip the samples, which has become widely used. [Fan et al. \(2021\)](#) proposed a shrinkage principle for low-rank matrix recovery with heavy-tailed data. Specifically, they truncated large heavy-tailed responses or covariates and used the clipped data in the least-squares method. Their theoretical results show that, under mild moment constraints, the robust estimator achieves a similar statistical error rate as in the case with sub-Gaussian tails. Subsequently, [Zhu and Zhou \(2021\)](#) adopted this robust methodology in generalized linear models and obtained good theoretical and numerical results. Inspired by [Fan et al. \(2021\)](#), [Wang and Tsay \(2023\)](#) and [Liu and Zhang \(2025\)](#) studied high-dimensional vector autoregression with heavy-tailed time series data. Both of their robust estimation procedures required clipping the data vector.

As more and more datasets appear in the form of tensors, conventional methods for studying regression problems based on vector and matrix-valued data are inadequate. Therefore, significant developments have been made in

tensor regression. For example, [Lu et al. \(2020\)](#) proposed an estimation procedure to estimate the tensor parameter in high-dimensional quantile regression. [Han et al. \(2022\)](#) introduces a unified statistical and computational framework for generalized low-rank tensor estimation under various probabilistic models, including sub-Gaussian tensor PCA, tensor regression, and Poisson and binomial tensor PCA. Under general deterministic conditions, they establish both statistical error bounds and linear convergence rates. The method is shown to achieve minimax optimal rates in several settings and is validated through simulations and real-data applications such as photon-limited imaging and click-through prediction.

To further fill the gap in robust estimation under tensor regression models and make progress in overcoming heavy-tailed errors from a statistical perspective, this paper investigates tensor regression models with heavy-tailed errors that have only finite second-order moments. By designing a robust gradient descent algorithm, we obtain a Huber-type robust estimator, which theoretically achieves the same optimal estimation error as in the case with sub-Gaussian noise, as shown in [Han et al. \(2022\)](#). We also optimize the sample complexity through careful proofs under mild constraints. The magnitudes of the robustification parameters used to control the bias and tail robustness are specified with respect to the dimensionality, rank, sample size, and finite second-order moments. Furthermore, to accommodate asymmetric additive errors, we generalize the Huber loss to a broader class of loss functions. Numerical simulations demonstrate that our estimator outperforms that of [Han et al. \(2022\)](#) under both homogeneous and heteroscedastic models. Finally, we apply our method to image recovery. Compared with the

original algorithm, the robust Huber loss-based algorithm shows a significant improvement in recovery performance.

The remainder of the paper is organized as follows: Section 2 gives the mathematical notation and definitions used in this paper. Section 3 presents our Huber-type parameter estimator for tensor regression with heavy-tailed errors and gives an upper bound in theory. Section 4 shows numerical experiments and empirical analysis to illustrate the validity of the methods in this paper. Section 5 gives the summary and discussion of this paper. Finally, the proofs of theorems are shown in Appendix.

## 2. Notation and definitions

For any positive integer  $n$ , we denote the set  $\{1, 2, \dots, n\}$  by  $[n]$ . Upper-case letters denote matrices, while calligraphic letters denote 3-order tensors. For two matrices  $X, Y \in \mathbb{R}^{p_1 \times p_2}$  and two tensors  $\mathcal{X}, \mathcal{Y} \in \mathbb{R}^{p_1 \times p_2 \times p_3}$ ,  $\langle X, Y \rangle := \text{tr}(X^\top Y)$  and  $\langle \mathcal{X}, \mathcal{Y} \rangle := \sum_{i,j,k} \mathcal{X}_{(i,j,k)} \mathcal{Y}_{(i,j,k)}$ . The Frobenius norms of  $X$  and  $\mathcal{X}$  are defined as  $\|X\|_F = \sqrt{\sum_{i,j} X_{(i,j)}^2}$  and  $\|\mathcal{X}\|_F = \sqrt{\sum_{i,j,k} \mathcal{X}_{(i,j,k)}^2}$ , respectively. The nuclear norm and spectral norm are defined as  $\|A\|_* = \text{tr}(\sqrt{A^\top A})$  and  $\|A\|_{\text{op}} = \sqrt{\lambda_{\max}(A^\top A)}$ . The unit Euclidean sphere on  $d$ -dimensional space is denoted by  $\mathbb{S}^{d-1}$ .  $\mathbb{O}^{p \times q} := \{\mathbf{U} \in \mathbb{R}^{p \times q} : \mathbf{U}^\top \mathbf{U} = \mathbf{I}_q\}$ . As a higher-order generalization of principal component analysis, the Tucker decomposition of a tensor is presented below:

**Definition 1** (Tensor Tucker decomposition). *For a given tensor  $\mathcal{A} \in \mathbb{R}^{p_1 \times p_2 \times p_3}$ , if there exist a tensor  $\mathcal{S} \in \mathbb{R}^{r_1 \times r_2 \times r_3}$  and a matrix  $\mathbf{U}_i \in \mathbb{O}^{p_i \times r_i}$  where  $r_i \leq p_i$ ,  $i \in [3]$  such that  $\mathcal{A} = \mathcal{S} \times_1 \mathbf{U}_1 \times_2 \mathbf{U}_2 \times_3 \mathbf{U}_3$ , then  $\mathcal{A}$  is said to be the rank-*

$(r_1, r_2, r_3)$  tensor, and  $\mathcal{S}$  is called the kernel tensor. For convenience, denote

$$\mathcal{A} = \mathcal{S} \times_1 \mathbf{U}_1 \times_2 \mathbf{U}_2 \times_3 \mathbf{U}_3 =: \llbracket \mathcal{S}; \mathbf{U}_1, \mathbf{U}_2, \mathbf{U}_3 \rrbracket,$$

where  $(\mathcal{S} \times_1 \mathbf{U}_1)_{i_1 i_2 i_3} := \sum_{j=1}^{r_1} \mathcal{S}_{ji_2 i_3} (\mathbf{U}_1)_{i_1 j}$ .  $\mathcal{S} \times_2 \mathbf{U}_2$  and  $\mathcal{S} \times_3 \mathbf{U}_3$  for  $\mathbf{U}_2 \in \mathbb{R}^{p_2 \times r_2}$ ,  $\mathbf{U}_3 \in \mathbb{R}^{p_3 \times r_3}$  are defined in a similar way.

Figure 1 shows a schematic diagram of the tensor Tucker decomposition.

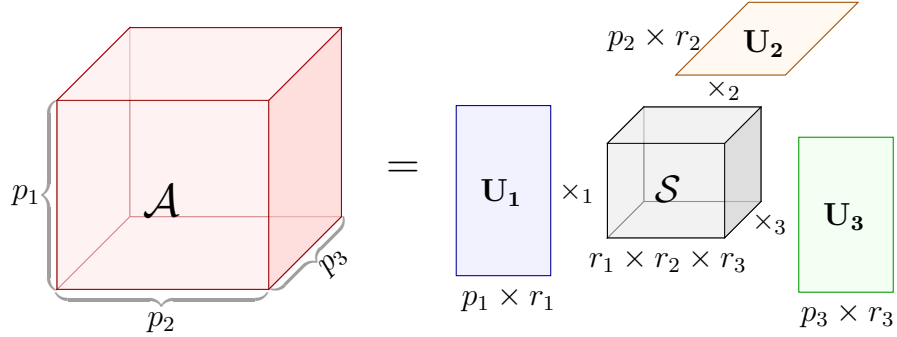


Figure 1: Tucker decomposition of tensor  $\mathcal{A} = \llbracket \mathcal{S}; \mathbf{U}_1, \mathbf{U}_2, \mathbf{U}_3 \rrbracket \in \mathbb{R}^{p_1 \times p_2 \times p_3}$ .

The matricization operator  $\mathcal{M}_k : \mathbb{R}^{p_1 \times p_2 \times p_3} \rightarrow \mathbb{R}^{p_k \times (p_{k+1} p_{k+2})}$  is defined as

$$[\mathcal{M}_k(\mathcal{A})]_{i_k, i_{k+1} + p_{k+1}(i_{k+2} - 1)} = \mathcal{A}_{i_1 i_2 i_3} \quad \text{for all } \mathcal{A} \in \mathbb{R}^{p_1 \times p_2 \times p_3},$$

where  $k + 1$  and  $k + 2$  are computed with modulo 3. The low-rank tensor can be Tucker decomposed by the following higher-order singular value decomposition algorithm proposed by [De Lathauwer et al. \(2000\)](#).

Let  $\kappa = \bar{\lambda}/\underline{\lambda}$ . Here, we define  $\bar{\lambda} := \max \{ \|\mathcal{M}_k(\mathcal{A}^*)\|_{\text{op}} : k \in [3] \}$  and  $\underline{\lambda} := \min \{ \sigma_{r_k}(\mathcal{M}_k(\mathcal{A}^*)) : k \in [3] \}$ . Furthermore, let  $\bar{p} = \max \{ p_k : k \in [3] \}$  and  $\bar{r} = \max \{ r_k : k \in [3] \}$ . For a differentiable function  $f : \mathbb{R}^{p_1 \times p_2 \times p_3} \rightarrow \mathbb{R}$ , we write  $\nabla f$  as its gradient function. Given two sequences  $\{a_n\}_{n=1}^{\infty}$  and

---

**Algorithm 1** High order singular value decomposition (HOSVD)

---

**Require:** rank- $(r_1, r_2, r_3)$  tensor  $\mathcal{Y} \in \mathbb{R}^{p_1 \times p_2 \times p_3}$ .

1:  $\mathbf{U}_k = \text{SVD}_{r_k}(\mathcal{M}_k(\mathcal{Y})), k = 1, 2, 3$

2:  $\mathcal{S} = \llbracket \mathcal{Y}; \mathbf{U}_1^\top, \mathbf{U}_2^\top, \mathbf{U}_3^\top \rrbracket$

**Ensure:**  $(\mathcal{S}, \mathbf{U}_1, \mathbf{U}_2, \mathbf{U}_3)$ .

---

$\{b_n\}_{n=1}^\infty$ , we use the notation  $a_n \asymp b_n$  if there exist positive constants  $C_1$  and  $C_2$  such that  $C_1 b_n \leq a_n \leq C_2 b_n$  for all  $n$ .

**Definition 2** (Huber loss (Huber, 1964)). *The Huber loss  $\ell_\varpi(\cdot)$  is defined as*

$$\ell_\varpi(x) = \begin{cases} x^2/2, & \text{if } |x| \leq \varpi; \\ \varpi|x| - \varpi^2/2, & \text{if } |x| > \varpi, \end{cases}$$

where  $\varpi$  is a robustification parameter which strikes a balance between the induced bias and tail robustness.

From the above definition, we obtain the following truncation function by deriving the Huber loss:

**Definition 3** (Clipping function). *Let  $\psi_\tau(\cdot)$  be a clipping function defined by*

$$\psi_\tau(x) = (|x| \wedge \tau) \text{sign}(x), \quad x \in \mathbb{R},$$

where  $\tau$  is a robustification parameter.

Figure 2 shows the image of Huber loss, squared loss and truncation function.

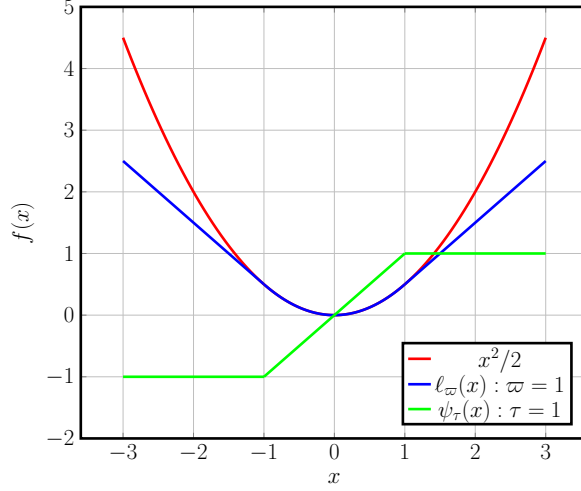


Figure 2: Illustration of Huber loss, square loss and truncation function.

### 3. Main result

#### 3.1. Model and theoretical results

Suppose  $n$  i.i.d. samples  $\{y_i, \mathcal{X}_i\}_{i=1}^n$  are generated from the following tensor regression:

$$y_i = \langle \mathcal{X}_i, \mathcal{A}^* \rangle + \varepsilon_i \quad \text{with} \quad \mathbb{E}(\varepsilon_i | \mathcal{X}_i) = 0 \quad \text{and} \quad M = \sqrt[k]{\mathbb{E}(\mathbb{E}(\varepsilon_i^2 | \mathcal{X}_i)^k)} < \infty, \quad (1)$$

where  $\mathcal{A}^* \in \mathbb{R}^{p_1 \times p_2 \times p_3}$  is a rank- $(r_1, r_2, r_3)$  tensor with  $r_k \ll p_k$ , to be estimated and  $\{\mathcal{X}_i\}_{i=1}^n$  are tensor covariates. Since the noise only possesses mild polynomial moment, the traditional least square method is not efficient in estimating the tensor parameter  $\mathcal{A}^*$  and sensitive to outliers and heavy-tailed data. In order to handle heavy-tailed noise, we propose to utilize Huber loss in Definition 2 and define the empirical loss function  $\mathcal{L}_w(\mathcal{A}) = \frac{1}{n} \sum_{i=1}^n \ell_w(y_i - \langle \mathcal{X}_i, \mathcal{A} \rangle)$ . We solve the following optimization prob-



lem to obtain a low-rank estimator for  $\mathcal{A}^*$  under the heavy-tailed setting:

$$(\widehat{\mathcal{S}}, \widehat{\mathbf{U}}_1, \widehat{\mathbf{U}}_2, \widehat{\mathbf{U}}_3) = \arg \min_{\mathcal{S}, \mathbf{U}_1, \mathbf{U}_2, \mathbf{U}_3} \left\{ \mathcal{L}_{\varpi}(\llbracket \mathcal{S}; \mathbf{U}_1, \mathbf{U}_2, \mathbf{U}_3 \rrbracket) + \frac{a}{2} \sum_{k=1}^3 \left\| \mathbf{U}_k^\top \mathbf{U}_k - b^2 \mathbf{I}_{r_k} \right\|_{\text{F}}^2 \right\},$$

where  $a, b > 0$  are tuning parameters. The regular term  $\frac{a}{2} \sum_{k=1}^3 \left\| \mathbf{U}_k^\top \mathbf{U}_k - b^2 \mathbf{I}_{r_k} \right\|_{\text{F}}^2$  ensures that in the process of using gradient descent method,  $\{\mathbf{U}_k\}_{k=1}^3$  are nonsingular without changing the minimum point. Before we employ the gradient descent method to get an excellent approximation of  $\llbracket \widehat{\mathcal{S}}; \widehat{\mathbf{U}}_1, \widehat{\mathbf{U}}_2, \widehat{\mathbf{U}}_3 \rrbracket$ , a reliable initialization is necessary. Han et al. (2022) constructed an unbiased estimator  $\frac{1}{n} \sum_{i=1}^n y_i \mathcal{X}_i$  based on the normality assumption for noise, but our noise distribution possesses a heavy-tail. Therefore, the response variable  $y_i$  needs to be trimmed via the clipping function defined in Definition 3.

By the above method, we use the following robust gradient descent algorithm to obtain our Huber-type robust estimator.

---

**Algorithm 2** The Robust Gradient Descent Algorithm

---

**Require:**  $\{y_i, \mathcal{X}_i\}_{i=1}^n$ , robustification parameters  $\tau$  and  $\varpi$ , tuning parameters  $a$  and  $b$ , step size  $\eta$ , the number of iteration  $T_{\max}$ .

- 1:  $\tilde{\mathcal{A}} = \frac{1}{n} \sum_{i=1}^n \psi_{\tau}(y_i) \mathcal{X}_i$
- 2:  $(\tilde{\mathcal{S}}, \tilde{\mathbf{U}}_1, \tilde{\mathbf{U}}_2, \tilde{\mathbf{U}}_3) = \text{HOSVD}(\tilde{\mathcal{A}})$  (HOSVD in Algorithm 1)
- 3: Let  $\mathbf{U}_k^{(0)} = b \tilde{\mathbf{U}}_k$  for  $k \in [3]$  and  $\mathcal{S}^{(0)} = \tilde{\mathcal{S}}/b^3$ .
- 4: **for**  $T = 0, 1, 2, \dots, T_{\max} - 1$  **do**
- 5:   For each  $k \in [3]$ , we compute the following equation:
- 6:    $\mathbf{U}_k^{(T+1)} = \mathbf{U}_k^{(T)} - \eta \left( \nabla_{\mathbf{U}_k} \mathcal{L}_{\varpi}(\mathcal{S}^{(T)}, \dots, \mathbf{U}_3^{(T)}) + a \mathbf{U}_k^{(T)} (\mathbf{U}_k^{(T)\top} \mathbf{U}_k^{(T)} - b^2 \mathbf{I}) \right).$
- 7:   Then:
- 8:    $\mathcal{S}^{(T+1)} = \mathcal{S}^{(T)} - \eta \nabla_{\mathcal{S}} \mathcal{L}_{\varpi}(\mathcal{S}^{(T)}, \mathbf{U}_1^{(T)}, \mathbf{U}_2^{(T)}, \mathbf{U}_3^{(T)})$ .
- 9: **end for**

**Ensure:**  $\mathcal{A}^{(T_{\max})} = \mathcal{S}^{(T_{\max})} \times_1 \mathbf{U}_1^{(T_{\max})} \times_2 \mathbf{U}_2^{(T_{\max})} \times_3 \mathbf{U}_3^{(T_{\max})}$ .

---

There are two main differences in Algorithm 2 compared with Han et al. (2022) such that it possesses the robustness against heavy-tailed errors of noise:

- (1) The initializer  $\tilde{\mathcal{A}}$  contains a robustification parameter  $\tau$  which clips the response  $\{y_i\}_{i=1}^n$ . the clipping technique has been successfully applied by Fan et al. (2021) and Zhu and Zhou (2021). Some specific benefits of doing so are stated in Remark 1.
- (2) We adopt Huber loss rather than the ordinary least squares considered by Han et al. (2022).

The statistical guarantee of  $\mathcal{A}^{(T_{\max})}$  is presented as follows.

**Theorem 1.** *Assume that the following conditions hold:*

- (1) *Let all entries of  $\mathcal{X}$  be i.i.d. sampled from sub-Gaussian distribution with mean-zero, variance-one and  $\|\mathcal{X}_{(j,k,l)}\|_{\psi_2} \leq K < \infty$ . Assume that  $\{\mathcal{X}_i\}_{i=1}^n$  are i. i. d. copies of  $\mathcal{X}$  and  $\{y_i\}_{i=1}^n$  are i.i.d. from (1).*
- (2) *Denote  $\bar{\lambda} := \max \{\|\mathcal{M}_k(\mathcal{A}^*)\|_{op} : k \in [3]\}$  and  $\underline{\lambda} := \min \{\sigma_{r_k}(\mathcal{M}_k(\mathcal{A}^*)) : k \in [3]\}$ , where  $\bar{p} = \max\{p_k : k \in [3]\}$  and  $\bar{r} = \max\{r_k : k \in [3]\}$ . There exist some positive constants  $\{c_i\}_{i=1}^3$  such that  $\underline{r} \geq c_1 \bar{r}$ ,  $M \leq c_2 \|\mathcal{A}^*\|_F^2$ ,  $\underline{r} \geq (\sqrt{\bar{p}} \log(\bar{p}))^{\frac{1}{3}}$  and  $\underline{\lambda} \geq c_3$ .*

*If  $\varpi \asymp_{K,k} (Mn/df)^{\frac{1}{2}}$ ,  $\tau \asymp_{K,k} (Rn/df)^{\frac{1}{2}}$ ,  $b \asymp \bar{\lambda}^{1/4}$  and  $a \asymp \frac{\bar{\lambda}}{\kappa^2}$  are chosen, then for  $\forall t > \log(13)$ , there exist positive constants  $c_0, c_1, c_2$  and  $\{C_i\}_{i=1}^5$  such that as long as  $\eta > c_0 \bar{\lambda}^{-\frac{3}{2}}$ ,*

$$n > C_1 \max \left\{ R^2 \bar{p}^{\frac{3}{2}} \bar{r}, R \kappa^2 \bar{p}^{\frac{3}{2}} \sqrt{\bar{r}}, \kappa^6 \bar{p} \bar{r}^2 \right\} \quad \text{and} \quad T_{\max} > C_2 \log \left( \frac{n \underline{\lambda}}{M df \kappa^4} \right),$$

with probability at least  $1 - 6 \exp(-c_1 \bar{p}) - 4 \exp(df(\log(13) - t)) - C_3 T_{\max} \exp(-C_4 df) - (T_{\max} + 4)e^{-\bar{p}^{\frac{3}{2}} \bar{r}} - 4\bar{p}^{-c_2}$ , we have

$$\|\mathcal{A}^{(T_{\max})} - \mathcal{A}^*\|_F < C_5 \kappa^2 \sqrt{Mdf/n} (\sqrt{t} + t),$$

where  $df := r_1 r_2 r_3 + \sum_{i=1}^3 p_i r_i$ ,  $\kappa = \bar{\lambda}/\lambda$  and  $R := \mathbb{E}[y_i^2]$ .

**Remark 1.** From Theorem 1, it follows that under the bounded second-order moments condition, our proposed estimator realizes the minmax optimal rate of convergence established by Han et al. (2022). On the other hand, the sample complexity  $n \gtrsim \bar{p}^{\frac{3}{2}} \bar{r}$  is also optimal if  $R$  is smaller than some fixed constant.

**Remark 2.** In the presence of heavy-tailed noises, the initializer  $\tilde{\mathcal{A}}$  offers some key virtues in both theoretical and numerical aspects. First, after appropriate truncation,  $\tilde{\mathcal{A}}$  has a non-asymptotic upper bound with an exponential-type exception probability. Therefore, it is a good initialization and well reflects the parameter tensor  $\mathcal{A}^*$ , which can provide a firm foundation for rank- $(r_1, r_2, r_3)$  estimation. Besides,  $\tilde{\mathcal{A}}$  can reduce the required number of iterations  $T_{\max}$  and enhance the stability of Algorithm 2.

**Remark 3.** The constraints on  $\underline{r}$  in condition (2) is easily satisfied. For example, if  $\bar{p} = 10^4$ , we only need  $\underline{r} \geq 10$ . Note that the scales of  $\tau$  and  $\varpi$  are related to the rank- $(r_1, r_2, r_3)$ , but in practice, the rank is often unknown. Therefore, in order to overcome this drawback, the estimate of  $\{r_k\}_{k=1}^3$  can be obtained by substituting the robust initial value  $\tilde{\mathcal{A}}$  into the rank selection

method of [Han et al. \(2022\)](#):

$$\hat{r}_k = \max \left\{ r : \sigma_r \left( \mathcal{M}_k(\tilde{\mathcal{A}}) \right) \geq c\delta_k \right\}, \quad k = 1, 2, 3,$$

where  $\delta_k := \text{Median} \left\{ \sigma_1 \left( \mathcal{M}_k(\tilde{\mathcal{A}}) \right), \dots, \sigma_{p_k} \left( \mathcal{M}_k(\tilde{\mathcal{A}}) \right) \right\}$  and  $c > 0$  are threshold levels.

**Remark 4.** Without considering the theoretical upper bound on the initial value  $\tilde{\mathcal{A}}$ , from the proof of Theorem 1, we can further obtain that when the error term has only finite  $(1 + \delta)$ -order moments, i.e., for  $\delta > 0$ ,  $M_\delta := \sqrt[k]{\mathbb{E} \left( \mathbb{E} (|\varepsilon_i|^{1+\delta} | \mathcal{X}_i)^k \right)} < \infty$ , if we choose  $\varpi \asymp_{K,k} \left( M_\delta^{1/k} n / df \right)^{\frac{1}{1+\delta}}$ , then we have

$$\left\| \mathcal{A}^{(T_{\max})} - \mathcal{A}^* \right\|_F \lesssim \kappa^2 M_\delta^{\frac{1}{k(1+\delta)}} \left( \frac{df}{n} \right)^{\frac{\delta}{1+\delta}} \text{ with high probability holds.}$$

It can be seen that the estimator has a smooth phase transition when  $0 < \delta < 1$ , which is similar to the adaptive Huber linear regression established by [Sun et al. \(2020\)](#). The simulation experiments in next section confirm the phenomenon.

The following corollary clarifies that as the sample size increases, we do not need the additional constraint to be added to the rank  $\underline{r}$ .

**Corollary 1.** Without the constraint condition  $\underline{r} \geq (\sqrt{\bar{p}} \log(\bar{p}))^{\frac{1}{3}}$ , the conclusion of Theorem 1 would still hold as long as

$$\tau \asymp_{K,k} \left\| \mathcal{A}^* \right\|_F (n/df)^{\frac{1}{2}}, \quad n \gtrsim \max \left\{ \kappa^4 \bar{p}^2 \log(\bar{p}), \kappa^4 \bar{p}^{\frac{3}{2}} \bar{r}^3, \kappa^6 \bar{p} \bar{r}^2 \right\}$$

are chosen.

### 3.2. Generalization of the loss function

Since different robust loss functions have different results when dealing with different types of heavy-tailed errors, in this subsection we generalize Huber loss to asymmetric loss functions (Man et al., 2024) which only need to satisfy the following assumptions:

**Assumption 1.** Let  $\ell_\varpi(x)$  fulfill the following conditions:

- (1)  $\ell_\varpi(x) = \varpi^2 \ell_1(x/\varpi)$ , where  $\ell_1 : \mathbb{R} \mapsto [0, \infty)$ ;
- (2)  $\ell'_1(0) = 0$ , for  $\forall x \in \mathbb{R}$ ,  $|\ell'_1(x)| \leq \min(c_1, |x|)$  and  $|\ell'_1(x) - x| \leq c_2 x^2$ ;
- (3)  $\ell''_1(0) = 1$  and for  $\forall |x| \leq c_3$ ,  $\ell''_1(x) \geq c_4$ , where  $\{c_i\}_{i=1}^4$  is a positive constant.

Assumption 1 contains a variety of loss functions such as Huber loss, Tukey's biweight loss

$$\ell_\varpi(x) = \begin{cases} \frac{\varpi^2}{6} \left(1 - \left(1 - \frac{x^2}{\varpi^2}\right)^3\right), & \text{if } |x| \leq \varpi, \\ \frac{\varpi^2}{6}, & \text{if } |x| > \varpi. \end{cases}$$

and Cauchy loss  $\ell_\varpi(x) = \frac{\varpi^2}{2} \log \left(1 + \frac{x^2}{\varpi^2}\right)$ . Using a robust approach similar to the previous section, define the empirical loss as  $\mathcal{L}_\varpi(\mathcal{A}) = \frac{1}{n} \sum_{i=1}^n \ell_\varpi(y_i - \langle \mathcal{X}_i, \mathcal{A} \rangle)$  and for the estimation of the initial values, we use the derivative function satisfying Assumption 1 to truncate the response variable and obtain  $\tilde{\mathcal{A}} = \frac{1}{n} \sum_{i=1}^n \ell'_\tau(y_i) \mathcal{X}_i$ . Based on this, the following theorem shows that the estimates produced by Algorithm 2 are still optimal in terms of the statistical error and sample complexity.

**Theorem 2.** *Under Assumption 1 and the conditions of Theorem 1, the following conclusion holds: For  $\forall t > \log(13)$ , with probability at least  $1 - 6 \exp(-c\bar{p}) - 4 \exp(df(\log(13) - t)) - C_2 T_{\max} \exp(-C_3 df) - (T_{\max} + 4)e^{-\bar{p}^{\frac{3}{2}\bar{r}}} - 4\bar{p}^{-c}$ , we have*

$$\|\mathcal{A}^{(T_{\max})} - \mathcal{A}^*\|_F < C_4 \kappa^2 \sqrt{Mdf/n} (\sqrt{t} + t).$$

## 4. Simulation analysis and application

### 4.1. Numerical experiments

In this section, we illustrate the statistical performance of Algorithm 2. Let  $r_1 = r_2 = r_3 = r$  and  $p_1 = p_2 = p_3 = p$  to facilitate simulation. The parameter tensor  $\mathcal{A}^* = \llbracket \mathcal{S}^*; \mathbf{U}_1^*, \mathbf{U}_2^*, \mathbf{U}_3^* \rrbracket$  is constructed by the following two steps:

- (1)  $\mathcal{S}^* = \lambda \mathcal{S} / \min \{\sigma_r(\mathcal{M}_k(\mathcal{S})) : k \in [3]\}$  where each entry of  $\mathcal{S}$  is drawn from  $\mathcal{N}(0, 1)$  and  $\lambda$  is a specified constant.
- (2) For each  $k \in [3]$ ,  $\mathbf{U}_k^*$  is top  $r$  eigenvectors of  $p$ -dimensional sample covariance matrix from 100 i.i.d. standard Gaussian random vectors. Tensor covariates  $\{\mathcal{X}_i\}_{i=1}^n$  have i.i.d. entries which are drawn from  $\mathcal{N}(0, 1)$ .

We compare Algorithm 2 with the algorithm of Han et al. (2022) and abbreviate them as RGD and GD, respectively. the results are shown in Figure 3 and Table 1. The experimental results are based on 200 independent repetitions. From Figure 3 with error bars, two algorithms possess similar statistical effects after 300 iterations, when the random noise follows standard

normal distribution. However, when the noise obeys a scaled Student's  $t$ -distribution with 2.1 degrees of freedom, RGD performs significantly better than GD. Table 1 presents parameter values in the experiments and shows that the initial value  $\tilde{\mathcal{A}}$  via using the truncation method outperforms the original estimator in terms of mean and standard deviation. There is a certain probability that the algorithm GD will fail to converge in 200 independently repeated experiments. The results in Figure 3 are calculated after eliminating these non-converging data, which show that our algorithm is more robust.

Table 1: Parameter values and initial values in Algorithm 2 for Figure 3 and the statistical performance of the initializer  $\tilde{\mathcal{A}}$ .

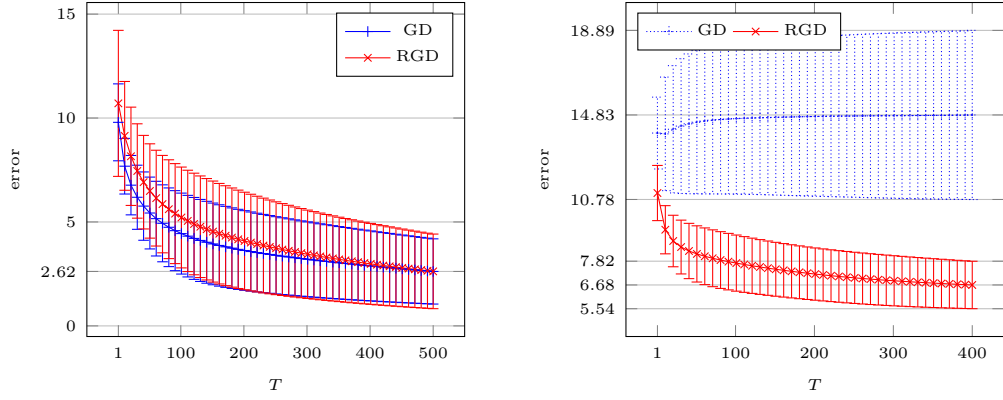
| Case | $\lambda$ | $\eta$             | $(a, b)$ | $(\tau, \varpi)$     | Initializer $\tilde{\mathcal{A}}$ | Failures | Algorithm |
|------|-----------|--------------------|----------|----------------------|-----------------------------------|----------|-----------|
| (a)  | 5         | $1 \times 10^{-3}$ | (5, 1)   | $(10, 3)\sqrt{n/df}$ | 40.04 <sub>(5.18)</sub>           | 0        | RGD       |
|      |           |                    |          | $+\infty$            | 48.92 <sub>(10.53)</sub>          | 3        | GD        |
| (b)  | 5         | $2 \times 10^{-3}$ | (5, 1)   | $(10, 5)\sqrt{n/df}$ | 31.84 <sub>(1.93)</sub>           | 0        | RGD       |
|      |           |                    |          | $+\infty$            | 55.06 <sub>(7.49)</sub>           | 14       | GD        |
| (c)  | 5         | $1 \times 10^{-3}$ | (5, 1)   | $(15, 5)\sqrt{n/df}$ | 46.47 <sub>(5.65)</sub>           | 0        | RGD       |
|      |           |                    |          | $+\infty$            | 64.47 <sub>(14.24)</sub>          | 4        | GD        |
| (d)  | 8         | $8 \times 10^{-4}$ | (5, 1)   | $(20, 8)\sqrt{n/df}$ | 61.30 <sub>(3.94)</sub>           | 0        | RGD       |
|      |           |                    |          | $+\infty$            | 78.83 <sub>(19.01)</sub>          | 0        | GD        |

In the above simulations we considered homogeneous model, i.e., the error distribution is independent of the covariates. In the next experiments, we consider evaluating the performance of RGD under the heteroscedastic model:

$$y_i = \langle \mathcal{X}_i, \mathcal{A}^* \rangle + 5c^{-1} (\langle \mathcal{X}_i, \mathcal{A}^* \rangle)^2 \varepsilon_i,$$

where the constant  $c = \sqrt{3} \|\mathcal{A}^*\|_F^2$  such that  $\mathbb{E} [c^{-2} (\langle \mathcal{X}_i, \mathcal{A}^* \rangle)^4] = 1$ . In

(a) :  $r = 3, p = 20, n = 1000, \mathcal{N}(0, 1)$  noise (b) :  $r = 3, p = 15, n = 1000, 10t_{2,1}$  noise



(c) :  $r = 3, p = 20, n = 2000, 10t_{2,1}$  noise (d) :  $r = 5, p = 30, n = 3000, 6t_{2,1}$  noise

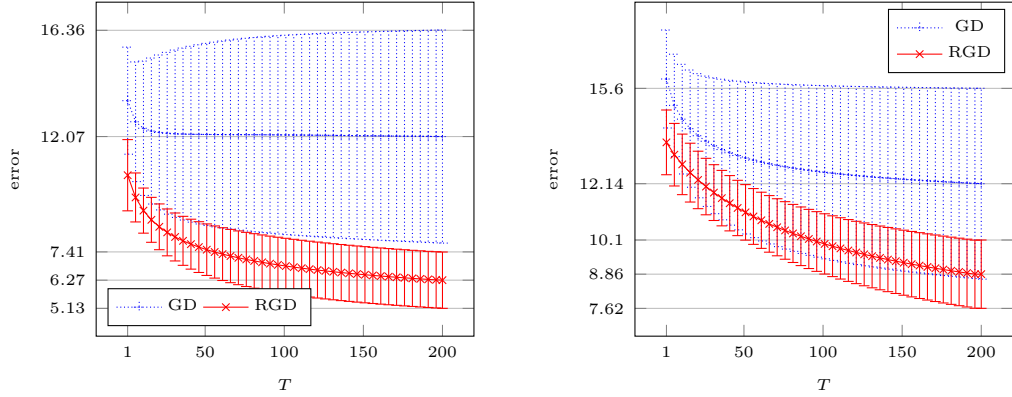


Figure 3: Comparison of statistical performance between RGD and GD.  $T$  and the error represent the number of iterations and  $\|\mathcal{A}^{(T)} - \mathcal{A}^*\|_F$  respectively.



order to model the various shapes of the error distribution, we consider the following three scenarios: (a)  $t_{2,1}$  distribution; (b) Pareto distribution; (c) LogNormal distribution. The composition of the tensor parameter  $\mathcal{A}^*$  is the same as the case of the homogeneous model and considers  $r = 3$  and  $p = 13$ . We choose  $\tau = 10\sqrt{n/df}$ ,  $\varpi = 5\sqrt{n/df}$  and  $\eta = 10^{-1}$ . Based on 200 independently repeated experiments, Tables 2 and 3 show that our method outperforms the least squares method for various heavy-tailed errors, including asymmetric ones.

Table 2: Simulation results under the heteroskedasticity model. Standard deviations are shown in parentheses.

| Case | Method | $n$             |                |                |                |
|------|--------|-----------------|----------------|----------------|----------------|
|      |        | 500             | 1000           | 1500           | 3000           |
| (a)  | RGD    | 5.6289 (1.762)  | 2.5250 (0.617) | 1.9901 (0.471) | 1.4469 (0.126) |
|      | GD     | 10.5183 (5.459) | 5.8554 (3.227) | 4.3039 (1.805) | 2.9340 (0.830) |
| (b)  | RGD    | 4.7553 (2.107)  | 2.1107 (0.767) | 1.4920 (0.294) | 1.0559 (0.088) |
|      | GD     | 7.8253 (5.238)  | 4.6653 (3.478) | 3.6750 (2.737) | 2.2123 (1.162) |
| (c)  | RGD    | 5.3948 (1.812)  | 2.5135 (0.653) | 1.8884 (0.332) | 1.3708 (0.127) |
|      | GD     | 9.0962 (4.277)  | 4.7237 (2.025) | 3.6291 (1.178) | 2.4001 (0.475) |

Table 3: The number of times the algorithm failed to converge in the experiments of Table 2.

| Case | Method | $n$ |      |      |      |
|------|--------|-----|------|------|------|
|      |        | 500 | 1000 | 1500 | 3000 |
| (a)  | RGD    | 0   | 0    | 0    | 0    |
|      | GD     | 17  | 10   | 12   | 10   |
| (b)  | RGD    | 0   | 0    | 0    | 0    |
|      | GD     | 11  | 3    | 11   | 8    |
| (c)  | RGD    | 0   | 0    | 0    | 0    |
|      | GD     | 10  | 10   | 10   | 9    |

#### 4.2. Phase transition phenomenon

According to Remark 4, the resulting estimator has the theoretical rate of order  $C(M_\delta, \kappa) \times \left(\frac{df}{n}\right)^{\min\{\frac{1}{2}, \frac{\delta}{1+\delta}\}}$  under Frobenius norm, where  $C(M_\delta, \kappa)$  is a positive constant depending only on  $M_\delta$  and  $\kappa$ . This means that when  $\delta < 1$ , the statistical error will increase sharply. To verify this phase transition phenomenon, we choose scaled Student's  $t_\nu$ -distributions with degrees of freedom  $\nu \in \{1.01, 1.1, 1.2, \dots, 2.9, 3\}$  as the error distribution. Take  $\delta = \nu - 1.01$  in the selection of truncation and robustification parameters when  $\nu \leq 2$ , otherwise  $\delta = 1$ . The statistical behavior of the adaptive Huber estimator is shown in Figure 4. For simplicity, the constant  $C(M_\delta, \kappa)$  in the theoretical bound is set as the fixed constant 13.4 for (a) and 13.2 for (b). The empirical curves in Figure 4 match the theoretical curves very well when  $\delta \leq 1$ . When  $\delta > 1$ , the statistical error still decreases gradually as  $\delta$  increases, which is consistent with the theory and intuitive expectation. Specifically, it is general knowledge that  $t_\nu \rightarrow \mathcal{N}(0, 1)$  as  $\nu \rightarrow \infty$  and  $M = \mathbb{E}[t_\nu^2] = \frac{\nu}{\nu-2} \xrightarrow{\nu \rightarrow \infty} 1$ . When the order of the moment grows,  $C(M, \kappa)$  will drop and the tail of the noise distribution is lighter. Therefore, the proposed estimator achieves a better statistical performance as expected than the case of the relatively small  $\delta$ .

#### 4.3. Image recovery

Since a two-dimensional image can be considered as a matrix, one approach to image compression is to approximate it by singular value decomposition using a low-rank matrix (see Recht et al., 2010; Wakin et al., 2006). In this section, we show the application of our algorithm in image restoration, which is used to verify the feasibility and effectiveness of the proposed

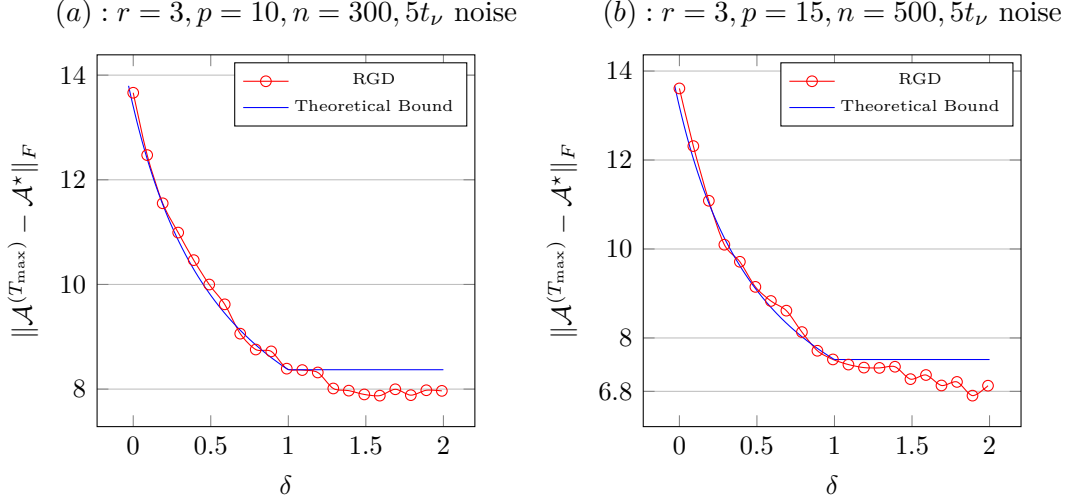


Figure 4: The trend of statistical errors with varying  $\delta$  where  $T_{\max} = 500$ .

method. Firstly, we consider the matrix version of (1), i.e., the matrix compressed sensing model:

$$y_i = \langle X_i, A^* \rangle + \varepsilon_i,$$

where  $X_i \in \mathbb{R}^{d_1 \times d_2}$  are covariates,  $A^* \in \mathbb{R}^{d_1 \times d_2}$  is a low-rank matrix parameter and  $\text{rank}(A^*) = r$ . Write  $A^*$  in the form of singular value decomposition denoted as  $A^* = U^* S^* V^{*\top}$  and obtain the low-rank estimate of  $A^*$  by solving the following optimization problem:

$$(\hat{S}, \hat{U}, \hat{V}) = \arg \min_{\hat{S}, \hat{U}, \hat{V}} \left\{ \mathcal{L}_{\varpi} (U S V^{\top}) + \frac{a}{2} \left( \|U^{\top} U - I_r\|_F^2 + \|V^{\top} V - I_r\|_F^2 \right) \right\}.$$

By the matrix version of Algorithm 2 and Theorem 1, it can be obtained that when  $n \gtrsim R^2 \bar{p} r$ , after enough iterations  $T_{\max}$ , we have with high probability

$$\|A^{(T_{\max})} - A^*\|_F \lesssim \kappa^2 \sqrt{M \bar{p} \bar{r} / n},$$

where  $R := \mathbb{E}[y_i^2]$ ,  $\kappa := \|A^*\|_{\text{op}} / \sigma_r(A^*)$ ,  $\bar{p} := d_1 \vee d_2$ ,  $\bar{r} := r$  and  $M := \sqrt[k]{\mathbb{E}(\mathbb{E}(\varepsilon_i^2 | X_i)^k)} < \infty$ . This is the same as error upper bound established by Negahban and Wainwright (2011) in sub-Gaussian noise. Next, we use each of three  $43 \times 53$  dimensional 0-1 matrices (Figure 1 of Kong et al. (2020)) as the parameter matrices of (1). As shown in the first row of images in Figure 5, we denote them as  $\{A_i^*\}_{i \in [3]}$  respectively. Each term of the covariates is chosen to be i.i.d. samples from  $\mathcal{N}(0, 1)$ . For the random error term, we consider three levels of scaled Student's  $t$ -distributions. Specifically, the noise is generated as  $\varepsilon_i = C \cdot T$ , where  $T \sim t_{2.1}$  is a random variable following a Student's  $t$ -distribution with 2.1 degrees of freedom. The scaling factor  $C$  is set to 1, 2, and 4, respectively, in each of the three experiments.

Table 4 shows the simulation results based on 200 repeated experiments, demonstrating that the proposed robust estimator has better statistical performance than the benchmark in terms of mean and standard deviation. We randomly select a dataset from the 200 experiments and plot the estimators of  $\{A_i^*\}_{i \in [3]}$ . These images are shown in Figure 5, where the images in the second row are the images reconstructed by the estimator proposed in this paper; The third row is the image reconstructed by the original least squares method. Figure 5 illustrates that our robust estimator outperforms the conventional least squares estimation.

Secondly, we confirm the superiority of the algorithm under heavy-tailed

noise by combining each channel of the four cigarette package images (Golden Dragon, Yellow Crane Tower, Hatamen and Hongtashan), each of which has the resolution of  $110 \times 70$  into a third-order tensor with appropriately scaling as a parameter of the model (i.e.,  $p_1 = 110, p_2 = 70, p_3 = 12$ ) (shown in Figure 6).

Each term of the covariates is chosen to be i.i.d. following  $\mathcal{N}(0, 1)$ , and the random error term  $\epsilon_i$  is generated as  $\varepsilon_i = 5 \cdot T$ , where  $T \sim t_{2.1}$  (a student's  $t$ -distribution with 2.1 degrees of freedom). The sample size is  $n = 25000$ . We choose  $r_1 = 60, r_2 = 40, r_3 = 12$  as the rank of the recovered tensor and the parameters are selected as  $a = 5, b = 1$  and  $\varpi = 100\sqrt{n/df}$ . The error  $\|A^{(T_{\max})} - A^*\|_F$  obtained after  $T_{\max} = 500$  iterations is 15.1514. The recovered parameter images as shown in Figure 7. The results show that Algorithm 2 can better recover the original image from its compressed measurements. For the least squares method, the algorithm will not converge.

Table 4: Comparison of estimation errors for two methods. Standard deviations are shown in parentheses.

| Method | $A_1^* (n = 5000)$ | $A_2^* (n = 10000)$ | $A_3^* (n = 10000)$ |
|--------|--------------------|---------------------|---------------------|
| RGD    | 0.6045 (0.0295)    | 0.9159 (0.0127)     | 0.6647 (0.0073)     |
| GD     | 1.1600 (0.8077)    | 1.2499 (0.1514)     | 0.8682 (0.0187)     |

#### 4.4. An application to Beijing air-quality dataset

We use the Beijing Air Quality dataset<sup>1</sup> to predict daily mean of PM2.5 concentrations and verify the superiority of our method. The feature matrix

<sup>1</sup>The Beijing Air Quality dataset (Du et al., 2021) can be accessed through the UCI repository at: <https://archive.ics.uci.edu/dataset/501/beijing+multi+site+air+quality+data>.

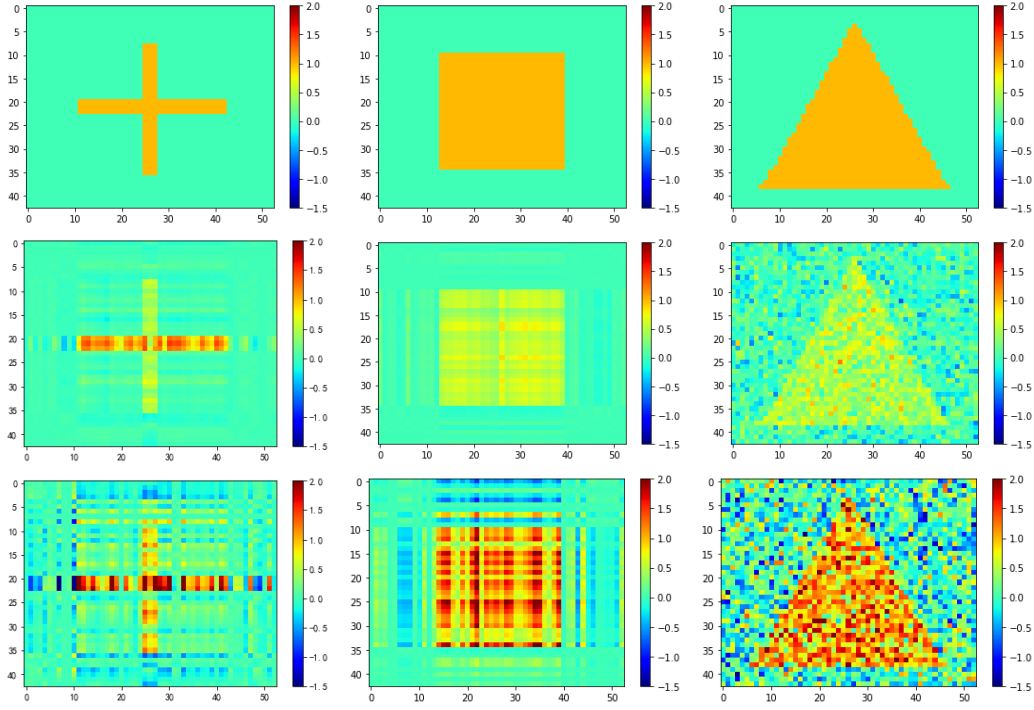


Figure 5: Images constructed by randomly selecting an experimental result from Table 4.



Figure 6: The images of cigarette package.

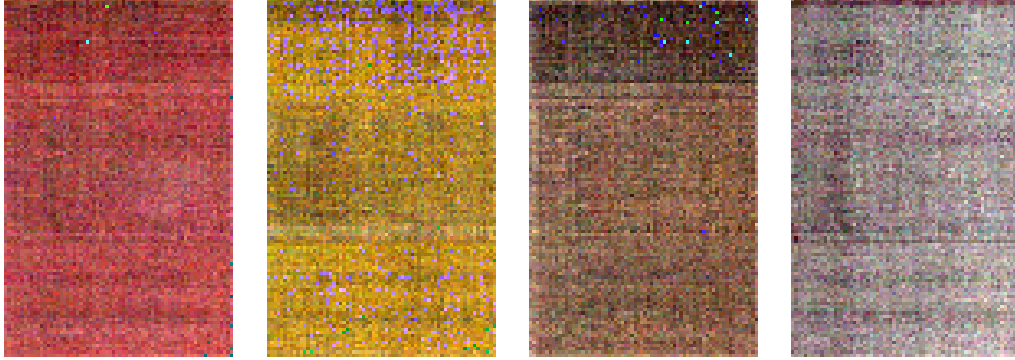


Figure 7: Recovered images.

$X_i$  encompasses 24-hourly measurements of eight covariates: the concentrations of  $\text{SO}_2$ ,  $\text{NO}_2$ ,  $\text{CO}$ , and  $\text{O}_3$ , along with the meteorological variables of temperature, atmospheric pressure, dew point, and wind speed. Thus,  $X_i \in \mathbb{R}^{24 \times 8}$ . The corresponding response variable  $y_i \in \mathbb{R}$  is the daily mean  $\text{PM}_{2.5}$  concentration. To apply our tensor regression framework to this problem, we treat the feature matrices  $X_i$  as 2nd-order tensors. Consequently, our general model specializes to the matrix regression setting, for which we aim to estimate a low-rank coefficient matrix  $A^* \in \mathbb{R}^{24 \times 8}$ . The complete dataset is collected from 12 monitoring stations. Each station contributes 1461 such daily observations  $(X_i, y_i)$ . In preprocessing, missing values in the features were imputed using their respective column means, after which all features were normalized.

We utilized data from the top five stations for testing our algorithm, assigning the first 1,200 samples to the training set and the subsequent 261 samples to the test set. We choose  $r = 5$  and select robustification parameters  $\tau$  and  $\varpi$  by 5-fold cross-validation. We use RMSE to measure the

performance of our method in test set, which is defined as

$$\text{RMSE} = \left\{ \frac{1}{n_{\text{test}}} \sum_{i=1}^{n_{\text{test}}} (y_i - \hat{y}_i)^2 \right\}^{1/2}.$$

The prediction results of our robust method (RGD) are shown in Figure 8. Notably, the standard gradient descent (GD) algorithm failed to converge on this dataset, and its results are therefore omitted. This failure is likely attributable to the presence of outliers or heavy-tailed distributions inherent in the real-world air quality data, which underscores the practical necessity of our robust methodology.

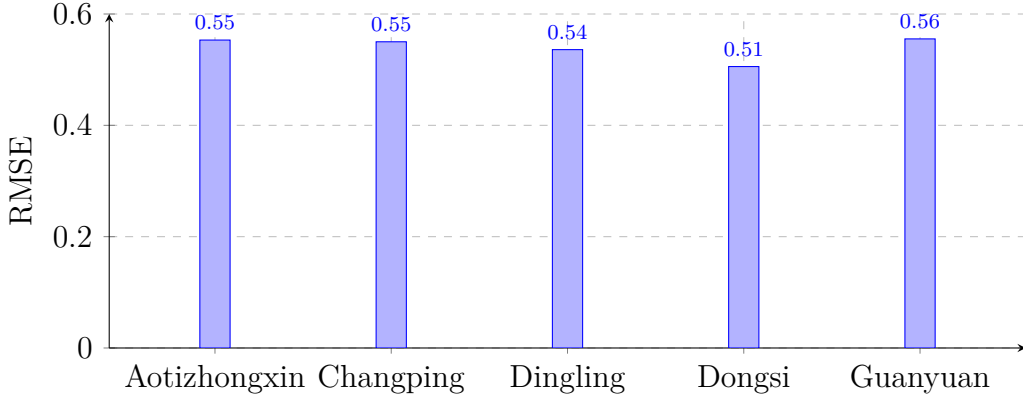


Figure 8: The prediction error of Algorithm 2.

## 5. Discussion

This paper proposes a robust parameter estimation framework for low-rank tensor regression model in the context of heavy-tailed errors, and theoretically establishes optimal convergence guarantee for only finite second-order moment noise. We also conduct simulations under both homogeneous



and heterogeneous models, demonstrating that the proposed robust estimator outperforms traditional methods in both scenarios. Finally, the method is applied to image recovery and Beijing air-quality dataset, yielding significant results. Furthermore, while this study focuses on parameter estimation for third-order tensor regression, our algorithm and results can also be extended to  $d$ -order low-rank tensor regression models. Specifically,

$$\begin{aligned} & (\widehat{\mathcal{S}}, \widehat{\mathbf{U}}_1, \widehat{\mathbf{U}}_2, \dots, \widehat{\mathbf{U}}_d) \\ &= \arg \min_{\mathcal{S}, \mathbf{U}_1, \mathbf{U}_2, \dots, \mathbf{U}_d} \left\{ \mathcal{L}_{\varpi}(\llbracket \mathcal{S}; \mathbf{U}_1, \mathbf{U}_2, \dots, \mathbf{U}_d \rrbracket) + \frac{a}{2} \sum_{k=1}^d \left\| \mathbf{U}_k^{\top} \mathbf{U}_k - b^2 \mathbf{I}_{r_k} \right\|_F^2 \right\}. \end{aligned}$$

Under conditions of Theorem 1, by choosing  $\varpi \asymp_{K,k} (Mn/df)^{\frac{1}{2}}$  and  $\tau \asymp_{K,k} (Rn/df)^{\frac{1}{2}}$ , after a sufficiently large number of iterations and sample sizes, the robust estimator yielded by Algorithm 2 has the error upper bound of

$$\left\| \mathcal{A}^{(T_{\max})} - \mathcal{A}^* \right\|_F \lesssim \kappa^2 \sqrt{Mdf/n}$$

with high probability, where the degrees of freedom are generalized to  $df := \prod_{k=1}^d r_k + \sum_{k=1}^d p_k r_k$ . The terms  $\bar{p} := \max\{p_k : k \in [d]\}$ ,  $\bar{r} := \max\{r_k : k \in [d]\}$  and  $\kappa$  are generalized accordingly from the 3rd-order case. On the other hand, our improved algorithm can also be used in the low SNR case (i.e., the case where  $\|\mathcal{A}^*\|_F^2 / \mathbb{E}[\varepsilon_i^2]$  is low). Due to space limitation, we do not continue the simulation demonstration in this paper.

There are still many areas in this paper that can be further improved and studied. The robust parameter  $\varpi$  of Huber loss in the paper can be

determined through cross-validation, while Wang et al. (2021) proposed a data-driven adaptive equation to determine the magnitude of the robust parameter in high-dimensional sparse linear regression model. Whether a similar adaptive method for solving the robustification parameter can be designed for low-rank tensor regression model is a question for future research. On the other hand, the assumption in Theorem 1 that each covariate term is i.i.d. is difficult to satisfy in practice. Whether this condition can be weakened is a very worthwhile research question.

### Declaration of competing interest

The authors declare that they have no known competing financial interests or personal relationships that could have appeared to influence the work reported in this paper.

### Funding

This research did not receive any specific grant from funding agencies in the public, commercial, or not-for-profit sectors.

### Appendix A. Proof of Theorem 1

For the convenience of the proof, we use the following mathematical notation: Since the loss function  $\mathcal{L}_\varpi(\mathcal{A}) = \frac{1}{n} \sum_{i=1}^n \ell_\varpi(y_i - \langle \mathcal{X}_i, \mathcal{A} \rangle)$ , denote  $\mathcal{X} : \mathbb{R}^{p_1 \times p_2 \times p_3} \rightarrow \mathbb{R}^n$  as the linear operator such that  $[\mathcal{X}(\mathcal{A})]_i = \langle \mathcal{X}_i, \mathcal{A} \rangle$  and  $\mathcal{X}^*$  is denoted as the adjoint operator of  $\mathcal{X}$ :

$$\mathcal{X}^*(x) = \frac{1}{n} \sum_{j=1}^n x_j \mathcal{X}_j, \quad x \in \mathbb{R}^n.$$

Then equation (1) can be rewritten as  $y = \mathcal{X}(\mathcal{A}^*) + \varepsilon \in \mathbb{R}^n$ ,  $\varepsilon := (\varepsilon_1, \dots, \varepsilon_n)^\top$  and the gradient of the loss function  $\nabla \mathcal{L}_\varpi(\mathcal{A})$  has the analytic form  $\mathcal{X}^*(\psi_\varpi(y - \mathcal{X}(\mathcal{A})))$ . For each iteration  $t = 0, 1, \dots, T_{\max}$ , define the measurement error:

$$E^{(t)} := \min_{\substack{\mathbf{R}_k \in \mathbb{O}^{p_k \times r_k} \\ k=1,2,3}} \left\{ \sum_{k=1}^3 \left\| \mathbf{U}_k^{(t)} - \mathbf{U}_k^* \mathbf{R}_k \right\|_F^2 + \left\| \mathcal{S}^{(t)} - \llbracket \mathcal{S}^*; \mathbf{R}_1^\top, \mathbf{R}_2^\top, \mathbf{R}_3^\top \rrbracket \right\|_F^2 \right\}.$$

With the above notation, we proceed to prove the theorem in the following two steps:

Step (1):  $E^{(0)} \lesssim \frac{\lambda^{1/2}}{\kappa^{3/2}}$ ;

Step (2): The loss function  $\mathcal{L}_\varpi(\mathcal{A}^{(T)})$  satisfies the constrained strong convexity condition with high probability within the closed set centered at  $\mathcal{A}^*$ .

Proof of step (1): According to the proof of Theorem 4.1 in [Han et al. \(2022\)](#), we have

$$\begin{aligned} & \left\| \mathcal{A}^{(0)} - \mathcal{A}^* \right\|_F \\ & \leq \left\| \mathcal{A}^* \times_1 \mathbb{P}_{\tilde{\mathbf{U}}_1} \times_2 \mathbb{P}_{\tilde{\mathbf{U}}_2} \times_3 \mathbb{P}_{\tilde{\mathbf{U}}_3} - \mathcal{A}^* \right\|_F + \left\| (\tilde{\mathcal{A}} - \mathcal{A}^*) \times_1 \mathbb{P}_{\tilde{\mathbf{U}}_1} \times_2 \mathbb{P}_{\tilde{\mathbf{U}}_2} \times_3 \mathbb{P}_{\tilde{\mathbf{U}}_3} \right\|_F \\ & \leq \sum_{k=1}^3 \left\| \mathcal{M}_k(\mathcal{A}^*) \right\|_{\text{op}} \cdot \left\| \sin \Theta(\tilde{\mathbf{U}}_k, \mathbf{U}_k) \right\|_F + \sup_{\substack{\mathcal{T} \in \mathbb{R}^{p_1 \times p_2 \times p_3} \\ \|\mathcal{T}\|_F \leq 1}} \left\langle \tilde{\mathcal{A}} - \mathcal{A}^*, \llbracket \mathcal{T}; \tilde{\mathbf{U}}_1^\top, \tilde{\mathbf{U}}_2^\top, \tilde{\mathbf{U}}_3^\top \rrbracket \right\rangle \\ & \leq \bar{\lambda} \sum_{k=1}^3 \sqrt{r_k} \left( \frac{\sigma_{r_k}(\mathbf{U}_k^\top \mathcal{M}_k(\tilde{\mathcal{A}})) \left\| \mathbf{U}_{k,\perp}^{*\top} \mathcal{M}_k(\tilde{\mathcal{A}}) \mathbb{P}_{(\mathbf{U}_k^{*\top} \mathcal{M}_k(\tilde{\mathcal{A}})^\top)^\top} \right\|_{\text{op}}}{\sigma_{r_k}^2(\mathbf{U}_k^\top \mathcal{M}_k(\tilde{\mathcal{A}})) - \sigma_{r_k+1}^2(\mathcal{M}_k(\tilde{\mathcal{A}}))} \wedge 1 \right) \\ & \quad + \sup_{\substack{\mathcal{T} \in \mathbb{R}^{p_1 \times p_2 \times p_3}, \|\mathcal{T}\|_F \leq 1 \\ \text{rank}(\mathcal{T}) \leq (r_1, r_2, r_3)}} \left\langle \tilde{\mathcal{A}} - \mathcal{A}^*, \mathcal{T} \right\rangle =: T_1 + T_2, \end{aligned}$$

where the last inequality follows from Proposition 1 of [Cai and Zhang \(2018\)](#).

We first find the upper bound of  $T_2$ : For a fixed  $\mathcal{T}$  with  $\|\mathcal{T}\|_F \leq 1$ ,

$$\begin{aligned} \left| \langle \tilde{\mathcal{A}} - \mathcal{A}^*, \mathcal{T} \rangle \right| &= \left| \sum_{(j,k,l)} \left( \tilde{\mathcal{A}}_{(i,j,k)} - \mathcal{A}^*_{(i,j,k)} \right) \mathcal{T}_{(j,k,l)} \right| = \left| \frac{1}{n} \sum_{i=1}^n \psi_\tau(y_i) z_i - \mathbb{E}[y_i z_i] \right| \\ &\leq \left| \frac{1}{n} \sum_{i=1}^n \psi_\tau(y_i) z_i - \mathbb{E}[\psi_\tau(y_i) z_i] \right| + |\mathbb{E}[\psi_\tau(y_i) z_i] - \mathbb{E}[y_i z_i]|, \end{aligned}$$

where  $z_i := \sum_{(j,k,l)} \mathcal{X}_{i(j,k,l)} \mathcal{T}_{(j,k,l)}$ . By the rotation invariance of sub-Gaussian random variable, we get that  $z_i$  is also a sub-Gaussian random variable with  $\|z_i\|_{\psi_2} = K$ . Therefore, since  $\sqrt[k]{\mathbb{E}|z_i|^k} \leq \sqrt{k}K$  for all  $k \geq 1$  and  $\|\text{vec}(\mathcal{X}_i)\|_{\psi_2} = K$ , we have for  $q \geq 2$ ,

$$\begin{aligned} \mathbb{E}|\psi_\tau(y_i) z_i|^q &\leq \tau^{q-2} \mathbb{E}|y_i^2 z_i^q| \leq 2 \cdot \tau^{q-2} \left( \mathbb{E}|\varepsilon_i|^2 |z_i^q| + \mathbb{E}|\langle \mathcal{X}_i, \mathcal{A}^* \rangle|^2 |z_i^q| \right) \\ &\leq 2\tau^{q-2} \left( \sqrt[k]{\mathbb{E} \left( \mathbb{E}(|\varepsilon_i|^2 | \mathcal{X}_i)^k \right)} \left( \mathbb{E}|z_i^{\frac{qk}{k-1}}| \right)^{\frac{k-1}{k}} + \sqrt{\mathbb{E}|\langle \mathcal{X}_i, \mathcal{A}^* \rangle|^4 \mathbb{E}|z_i^{2q}|} \right) \\ &\leq 2\tau^{q-2} \left( M \left( \frac{K^2 q k}{k-1} \right)^{q/2} + 4K^2 \|\mathcal{A}^*\|_F^2 (K\sqrt{2q})^q \right) \\ &\leq 2q! M \left( eK\tau \sqrt{\frac{2k}{k-1}} \right)^{q-2}, \end{aligned} \tag{A.1}$$

where the last inequality is derived from Stirling's inequality and  $\|\mathcal{A}^*\|_F^2 \leq \mathbb{E}|\langle \mathcal{X}_i, \mathcal{A}^* \rangle|^2 \leq \mathbb{E}[y_i^2] \leq R$ . By Bernstein's inequality, we obtain that there exists an absolute constant  $C$  depending on  $K, k$  and  $c$  such that

$$\mathbb{P} \left( \left| \frac{1}{n} \sum_{i=1}^n \psi_\tau(y_i) z_i - \mathbb{E} \psi_\tau(y_i) z_i \right| \leq C \sqrt{\frac{Rt}{n}} + C \frac{\tau t}{n} \right) \geq 1 - 2e^{-t}. \tag{A.2}$$

For the second term, we have

$$\begin{aligned}
& |\mathbb{E}[\psi_\tau(y_i)z_i] - \mathbb{E}[y_iz_i]| = |\mathbb{E}[(\psi_\tau(y_i) - y_i)z_i]| \\
&= \left| \mathbb{E} \left[ (\tau \operatorname{sign}(y_i) - y_i) 1_{\{|y_i| > \tau\}} z_i \right] \right| \\
&\leq \mathbb{E} \left[ |y_i| 1_{\{|y_i| > \tau\}} |z_i| \right] + \tau \mathbb{E} \left[ 1_{\{|y_i| > \tau\}} |z_i| \right] \\
&\leq \sqrt{\mathbb{E}[y_i^2 z_i^2] \mathbb{P}(|y_i| > \tau)} + \tau \sqrt{\mathbb{E}[z_i^2] \mathbb{P}(|y_i| > \tau)} \\
&\leq \frac{\sqrt{\mathbb{E}[y_i^2 z_i^2] \mathbb{E}[y_i^2]}}{\tau} + \frac{\tau \sqrt{\mathbb{E}[z_i^2] \mathbb{E}[y_i^2]}}{\tau} \\
&\lesssim \frac{\sqrt{R \cdot R}}{\tau} + \sqrt{1 \cdot R} \lesssim R/\tau.
\end{aligned} \tag{A.3}$$

Therefore, by combining (A.2) with (A.3), there is a constant  $C_1$  depending only on  $K, k$  and  $c$  such that

$$\mathbb{P} \left( \left| \langle \tilde{\mathcal{A}} - \mathcal{A}^*, \mathcal{T} \rangle \right| \leq C_1 \sqrt{\frac{Rt}{n}} + C_1 \frac{\tau t}{n} + C_1 R/\tau \right) \geq 1 - 2e^{-t}.$$

By following the  $\frac{1}{3}$ -net argument in Lemma E.5 of [Han et al. \(2022\)](#), we can obtain that with probability at least  $1 - 2 \exp(df(\log(13) - t))$ ,

$$\sup_{\substack{\mathcal{T} \in \mathbb{R}^{p_1 \times p_2 \times p_3}, \|\mathcal{T}\|_{\mathbb{F}} \leq 1 \\ \operatorname{rank}(\mathcal{T}) \leq (r_1, r_2, r_3)}} \langle \tilde{\mathcal{A}} - \mathcal{A}^*, \mathcal{T} \rangle \leq C \sqrt{\frac{Mdf \times t}{n}} + C \frac{\tau df \times t}{n} + C_1 M/\tau,$$

where  $C_2$  is an absolute constant. By choosing  $\tau \asymp_{K,k} (Mn/df)^{\frac{1}{2}}$  and  $t >$

log(13), the above inequality changes into

$$\mathbb{P} \left( \sup_{\substack{\mathcal{T} \in \mathbb{R}^{p_1 \times p_2 \times p_3}, \|\mathcal{T}\|_{\mathbb{F}} \leq 1 \\ \text{rank}(\mathcal{T}) \leq (r_1, r_2, r_3)}} \langle \tilde{\mathcal{A}} - \mathcal{A}^*, \mathcal{T} \rangle \leq C_3 \sqrt{\frac{Rdf}{n}} \right) \geq 1 - 2 \exp(-C_4 df). \quad (\text{A.4})$$

Next, we solve for the upper bound of  $T_1$ . In the proof of Theorem 4 in [Zhang et al. \(2020\)](#), via applying Lemma 2 and Lemma 3, we obtain that there exists a positive constant  $c < 1$  such that with probability at least  $1 - 2e^{-cp_1} - 4e^{-t}$ , the following inequality holds:

$$\begin{aligned} & \frac{\sigma_{r_k} \left( \mathbf{U}_k^{*\top} \mathcal{M}_k(\tilde{\mathcal{A}}) \right) \left\| \mathbf{U}_{k\perp}^{*\top} \mathcal{M}_k(\tilde{\mathcal{A}}) \mathbb{P}_{(\mathbf{U}_k^{*\top} \mathcal{M}_k(\tilde{\mathcal{A}})^\top)^\top} \right\|_{\text{op}}}{\sigma_{r_k}^2 \left( \mathbf{U}_k^{*\top} \mathcal{M}_k(\tilde{\mathcal{A}}) \right) - \sigma_{r_{k+1}}^2 \left( \mathcal{M}_k(\tilde{\mathcal{A}}) \right)} \\ & \lesssim \frac{\left( (1-c)\sigma_{r_1}(\mathcal{M}_k(\mathcal{A}^*)) + a_1 \sqrt{p_2 p_3 / n} \right) a_1 \sqrt{p_1 / n}}{\left( (1-c)\sigma_{r_1}(\mathcal{M}_k(\mathcal{A}^*)) + a_2 \sqrt{p_2 p_3 / n} \right)^2 - a_3(p_2 p_3 + C \sqrt{p_1 p_2 p_3})} \\ & \lesssim \frac{(1-c)\sigma_{r_1}(\mathcal{M}_k(\mathcal{A}^*)) a_1 \sqrt{p_1 / n} + a_1^2 \sqrt{p_1 p_2 p_3} / n}{(1-c)^2 \sigma_{r_1}^2(\mathcal{M}_k(\mathcal{A}^*)) - 2\tau^2 \sqrt{\frac{2t}{n}} p_2 p_3 / n - C \frac{\mathbb{E}[\eta_i^2] + \tau^2 \sqrt{2t/n}}{n} \sqrt{p_1 p_2 p_3}} \\ & \lesssim \frac{(1-c)\sigma_{r_1}(\mathcal{M}_k(\mathcal{A}^*)) \left( \|\mathcal{A}^*\|_F \sqrt{p_1 / n} + \sqrt{\frac{4t}{n}} \|\mathcal{A}^*\|_F \sqrt{p_1 / df} \right) + \|\mathcal{A}^*\|_F^2 \frac{\bar{p}^{3/2}}{n} + \frac{\|\mathcal{A}^*\|_F^2}{df} \sqrt{\frac{2t \bar{p}^3}{n}}}{\sigma_{r_1}^2(\mathcal{M}_k(\mathcal{A}^*))}, \end{aligned} \quad (\text{A.5})$$

where  $a_1 := \sqrt{\|\mathcal{A}^*\|_F^2 + \tau^2 \sqrt{\frac{2t}{n}}}$ ,  $a_2 := \sqrt{\mathbb{E}[\psi_\tau(\eta_i)^2] - \tau^2 \sqrt{\frac{2t}{n}}}$  and  $a_3 := \frac{\mathbb{E}[\psi_\tau(\eta_i)^2] + \tau^2 \sqrt{\frac{2t}{n}}}{n}$ .

Therefore, combining (A.5) with (A.4), by the union bound, we obtain that when  $t = c \log(\bar{p})$ , with probability at least  $1 - 4\bar{p}^{-c} - 6 \exp(-c\bar{p}) - 2 \exp(C_5 df)$

such that

$$\begin{aligned}
& \|\mathcal{A}^{(0)} - \mathcal{A}^*\|_F \\
& \leq C_4 \|\mathcal{A}^*\|_F \sqrt{\frac{df}{n}} + C_4 \bar{\lambda} \sqrt{\bar{r}} \|\mathcal{A}^*\|_F \\
& \quad \times \frac{(1-c)\sigma_{r_1}(\mathcal{M}_k(\mathcal{A}^*)) \left( \sqrt{\bar{p}/n} + \sqrt[4]{\frac{2\log(\bar{p})}{n}} \sqrt{\bar{p}/df} \right) + \|\mathcal{A}^*\|_F \frac{\bar{p}^{3/2}}{n} + \frac{\|\mathcal{A}^*\|_F}{df} \sqrt{\frac{2\log(\bar{p})\bar{p}^3}{n}}}{\sigma_{r_1}^2(\mathcal{M}_k(\mathcal{A}^*))}.
\end{aligned}$$

Because of the inequalities  $(x+y)^2 \leq 2x^2 + 2y^2$  and  $n \gtrsim \max \left\{ R\kappa^2 \bar{p}^{\frac{3}{2}} \sqrt{\bar{r}}, \kappa^6 \bar{p} \bar{r}^2 \right\}$ , by Lemma E.2 of [Han et al. \(2022\)](#), we have

$$\begin{aligned}
E^{(0)} & \leq 11\kappa^2 b^{-6} \|\mathcal{A}^{(0)} - \mathcal{A}^*\|_F^2 \\
& \lesssim \kappa^2 b^{-6} \bar{\lambda}^2 \bar{r} \left( \frac{\frac{\|\mathcal{A}^*\|_F^2 p_1}{n} + \sqrt{\frac{2t}{n}} \frac{p_1 \|\mathcal{A}^*\|_F^2}{df}}{\sigma_{r_1}^2(\mathcal{M}_k(\mathcal{A}^*))} + \frac{\frac{\|\mathcal{A}^*\|_F^4 \bar{p}^3}{n^2} + \frac{2\|\mathcal{A}^*\|_F^4 t \bar{p}^3}{df^2 n}}{\sigma_{r_1}^4(\mathcal{M}_k(\mathcal{A}^*))} \right) \lesssim \frac{\lambda^{1/2}}{\kappa^{3/2}}.
\end{aligned}$$

Proof of step (2): We generalize Lemma 4 of [Sun et al. \(2020\)](#) to present that the restricted strong convexity condition is satisfied for the Huber loss under the set  $\mathcal{C}(R) := \{\mathcal{A} \in \mathbb{R}^{p_1 \times p_2 \times p_3} : \|\mathcal{A} - \mathcal{A}^*\|_F \leq R, \text{rank}(\mathcal{A} - \mathcal{A}^*) \leq 2(r_1, r_2, r_3)\}$  with high probability.

**Lemma 1.** *Suppose that all entries of  $\mathcal{X}_i$  are i.i.d. sampled from sub-Gaussian distribution with mean-zero and variance-one. Then for all  $\mathcal{A} \in \mathcal{C}(R)$ , as long as the following conditions hold:*

$$\varpi \gtrsim \max \left\{ (4M)^{\frac{1}{2}}, 4c_1^2 R \right\}, \quad n \gtrsim (\varpi/R)^2 \left( \bar{p}^{3/2} \bar{r} + t \right),$$

*we have that*

$$\mathbb{P} \left( \langle \nabla \mathcal{L}_\varpi(\mathcal{A}) - \nabla \mathcal{L}_\varpi(\mathcal{A}^*), \mathcal{A} - \mathcal{A}^* \rangle \geq \frac{4}{5} \|\mathcal{A} - \mathcal{A}^*\|_F^2 \right) \geq 1 - e^{-t},$$

where  $c_1 \geq \sup_{\substack{\mathcal{V} \in \mathbb{R}^{p_1 \times p_2 \times p_3} \\ \|\mathcal{V}\|_F \leq 1}} (\mathbb{E} \langle \mathcal{V}, \mathcal{X}_i \rangle^4)^{1/4}$  is a positive constant.

*Proof.* The difference with the proof of Lemma 4 in [Sun et al. \(2020\)](#) is that we denote

$$\mathbb{Z}_{\mathcal{A}} := \frac{\tau}{2Rn} \sum_{i=1}^n G'_i \frac{\langle \mathcal{X}_i, \mathcal{A} - \mathcal{A}^* \rangle}{\|\mathcal{A} - \mathcal{A}^*\|_F},$$

where  $G'_i \stackrel{i.i.d.}{\sim} N(0, 1)$  and are independent with  $\mathcal{X}_i$ . Because  $G'_i \mathcal{X}_{i(j,k,l)}$  is a sub-exponential random variable with  $\|G'_i \mathcal{X}_{i(j,k,l)}\|_{\psi_1} = K$ , by Theorem 2.5 of [Boucheron et al. \(2013\)](#), we have that

$$\mathbb{E} \left[ \left| \frac{1}{n} \sum_{i=1}^n G'_i \mathcal{X}_{i(j,k,l)} \right|^2 \right] \lesssim \frac{K^2}{n} \quad \text{and} \quad \mathbb{E} \left[ \left| \frac{1}{n} \sum_{i=1}^n G'_i \mathcal{X}_{i(j,k,l)} \right|^4 \right] \lesssim \frac{K^4}{n^2}.$$

For  $\{A_i\}_{i \in [\lceil \sqrt{p_3} \rceil]} \subset \mathbb{R}^{p_1 \times p_2 \lceil \sqrt{p_3} \rceil}$ , denote

$$\overline{\mathcal{M}} \left( \frac{1}{n} \sum_{i=1}^n G'_i \mathcal{X}_i \right) = \begin{bmatrix} A_1^\top & A_2^\top & \cdots & A_{\lceil \sqrt{p_3} \rceil}^\top \end{bmatrix}^\top \in \mathbb{R}^{p_1 \lceil \sqrt{p_3} \rceil \times p_2 \lceil \sqrt{p_3} \rceil},$$

where

$$\begin{bmatrix} A_1 & A_2 & \cdots & A_{\lceil \sqrt{p_3} \rceil} \end{bmatrix} = \begin{bmatrix} \mathcal{M}_1 \left( \frac{1}{n} \sum_{i=1}^n G'_i \mathcal{X}_i \right) & \mathbf{0}_{p_1 \times p_2 (\lceil \sqrt{p_3} \rceil^2 - p_3)} \end{bmatrix}.$$



Then, by [Latała \(2005\)](#), it follows that

$$\begin{aligned} \mathbb{E} \left[ \left\| \overline{\mathcal{M}} \left( \frac{1}{n} \sum_{i=1}^n G'_i \mathcal{X}_i \right) \right\|_{\text{op}} \right] &\lesssim_K \sqrt{\frac{p_2 \lceil \sqrt{p_3} \rceil}{n}} + \sqrt{\frac{p_1 \lceil \sqrt{p_3} \rceil}{n}} + \sqrt[4]{\frac{p_1 \lceil \sqrt{p_3} \rceil^2 p_3}{n^2}} \\ &\lesssim_K \sqrt{\frac{\bar{p}^{3/2}}{n}}. \end{aligned} \quad (\text{A.6})$$

Because of  $\text{rank}(\overline{\mathcal{M}}(\mathcal{A} - \mathcal{A}^*)) \leq 2r_1$ , we get

$$\begin{aligned} &\mathbb{E} \left\{ \sup_{\mathcal{A} \in \mathcal{C}(R')} \mathbb{Z}_{\mathcal{A}} \right\} \\ &= \frac{\varpi}{2R'} \mathbb{E} \left\{ \sup_{\mathcal{A} \in \mathcal{C}(R')} \frac{\langle \overline{\mathcal{M}} \left( \frac{1}{n} \sum_{i=1}^n G'_i \mathcal{X}_i \right), \overline{\mathcal{M}}(\mathcal{A} - \mathcal{A}^*) \rangle}{\|\mathcal{A} - \mathcal{A}^*\|_F} \right\} \\ &\lesssim \frac{\varpi}{R'} \mathbb{E} \left\{ \sup_{\mathcal{A} \in \mathcal{C}(R')} \left\| \overline{\mathcal{M}} \left( \frac{1}{n} \sum_{i=1}^n G'_i \mathcal{X}_i \right) \right\|_{\text{op}} \frac{\|\overline{\mathcal{M}}(\mathcal{A} - \mathcal{A}^*)\|_*}{\|\mathcal{A} - \mathcal{A}^*\|_F} \right\} \\ &\lesssim \frac{\varpi}{R'} \mathbb{E} \left\{ \left\| \overline{\mathcal{M}} \left( \frac{1}{n} \sum_{i=1}^n G'_i \mathcal{X}_i \right) \right\|_{\text{op}} \sqrt{r_1} \right\} \stackrel{(\text{A.6})}{\lesssim_K} \frac{\varpi}{R'} \sqrt{\frac{\bar{p}^{3/2} \bar{r}}{n}}, \end{aligned}$$

where the first and second inequalities come from  $\langle A, B \rangle \leq \|A\|_{\text{op}} \|B\|_*$  where  $A$  and  $B$  are any two matrices of the same size, and  $\|A\|_* \leq \sqrt{\text{rank}(A)} \|A\|_F$ .  $\square$

Based on Lemma 1 and  $\varpi \asymp_{K,k} (Mn/df)^{\frac{1}{2}}$ , we can get that at  $T$ -th iteration,  $\mathcal{A}^{(T)} \in \mathcal{C}(\varpi)$  and (D.12) in the proof of Theorem 4 in [Han et al. \(2022\)](#) is satisfied with high probability. With the above two steps as a basis, by  $\mathcal{A}^{(T)} \in \mathcal{C}(R)$ , by Lemma E.6 of [Han et al. \(2022\)](#), we obtain that as long

as  $n \gtrsim df$ , for any rank- $(r_1, r_2, r_3)$  tensor,

$$\begin{aligned}
& \left| \left\langle \mathcal{X}', \nabla \mathcal{L}_{\varpi}(\mathcal{A}^{(T)}) - \nabla \mathcal{L}_{\varpi}(\mathcal{A}^*) \right\rangle \right| \\
&= \left| \left\langle \frac{1}{n} \mathcal{X}(\mathcal{X}'), \psi_{\varpi}(\mathcal{X}(\mathcal{A}^{(T)}) - y) - \psi_{\varpi}(\varepsilon) \right\rangle \right| \\
&\leq \frac{1}{n} \|\mathcal{X}(\mathcal{X}')\|_2 \|\psi_{\varpi}(\mathcal{X}(\mathcal{A}^{(T)}) - y) - \psi_{\varpi}(\varepsilon)\|_2 \\
&\leq \frac{11}{9\sqrt{n}} \|\mathcal{X}'\|_F \|\mathcal{X}(\mathcal{A}^{(T)} - \mathcal{A}^*)\|_2 \leq \frac{121}{81} \|\mathcal{X}'\|_F \|\mathcal{A}^{(T)} - \mathcal{A}^*\|_F \\
&< \frac{3}{2} \|\mathcal{X}'\|_F \|\mathcal{A}^{(T)} - \mathcal{A}^*\|_F
\end{aligned}$$

with probability at least  $1 - C_{10} \exp(-C_{11} df)$ . Finally, by following the lines of the proof of Theorem 4.2 in [Han et al. \(2022\)](#), we obtain that

$$\|\mathcal{A}^{(T+1)} - \mathcal{A}^*\|_F^2 \leq C_{12} \left( \kappa^4 \xi^2 + \left(1 - \frac{\eta_0}{1000\kappa^2}\right)^{T+1} \kappa^2 \|\mathcal{A}^{(0)} - \mathcal{A}^*\|_F^2 \right),$$

where  $\xi := \sup_{\substack{\mathcal{T} \in \mathbb{R}^{p_1 \times p_2 \times p_3}, \|\mathcal{T}\|_F \leq 1, \\ \text{rank}(\mathcal{T}) \leq (r_1, r_2, r_3)}} |\langle \nabla \mathcal{L}_{\varpi}(\varepsilon_i), \mathcal{T} \rangle|$  and  $\eta_0 < c$ , and  $c$  is a small positive constant. Therefore, as long as  $T_{\max} \gtrsim \log\left(\frac{\|\mathcal{A}^{(0)} - \mathcal{A}^*\|_F}{\kappa \xi}\right) / \log\left(\frac{\kappa^2}{\kappa^2 - 2\rho\eta_0}\right)$ , we have

$$\|\mathcal{A}^{(T_{\max})} - \mathcal{A}^*\|_F \lesssim \kappa^2 \xi.$$

By the proof of Theorem 2, it follows that

$$\mathbb{P} \left( \|\mathcal{A}^{(T_{\max})} - \mathcal{A}^*\|_F \lesssim \kappa^2 \left( \frac{Mdf}{n} \right)^{\frac{1}{2}} (\sqrt{t} + t) \right) \geq 1 - 2 \exp(df(\log(13) - t)).$$

## Appendix B. Proof of Theorem 2

Since

$$\begin{aligned}\xi &:= \sup_{\substack{\mathcal{T} \in \mathbb{R}^{p_1 \times p_2 \times p_3}, \|\mathcal{T}\|_{\text{F}} \leq 1, \\ \text{rank}(\mathcal{T}) \leq (r_1, r_2, r_3)}} |\langle \nabla \mathcal{L}_{\varpi}(\varepsilon_i), \mathcal{T} \rangle| \\ &= \sup_{\substack{\mathcal{T} \in \mathbb{R}^{p_1 \times p_2 \times p_3}, \|\mathcal{T}\|_{\text{F}} \leq 1, \\ \text{rank}(\mathcal{T}) \leq (r_1, r_2, r_3)}} \left| \left\langle \frac{1}{n} \sum_{i=1}^n \ell'_{\varpi}(\varepsilon_i) \mathcal{X}_i, \mathcal{T} \right\rangle \right|\end{aligned}$$

and  $\mathbb{E} [\varepsilon_i \mathcal{X}_{i(j,k,l)}] = \mathbb{E} [\mathcal{X}_{i(j,k,l)} \mathbb{E} [\varepsilon_i | \mathcal{X}_{i(j,k,l)}]] = 0$  for  $(j, k, l) \in [p_1] \times [p_2] \times [p_3]$ , we have

$$\begin{aligned}\left| \frac{1}{n} \sum_{i=1}^n \ell'_{\varpi}(\varepsilon_i) \sum_{(j,k,l)} \mathcal{X}_{i(j,k,l)} \mathcal{T}_{(j,k,l)} \right| &\leq |\mathbb{E} [\ell'_{\varpi}(\varepsilon_i) z_i] - \mathbb{E} [\varepsilon_i z_i]| \\ &\quad + \left| \frac{1}{n} \sum_{i=1}^n \ell'_{\varpi}(\varepsilon_i) z_i - \mathbb{E} [\ell'_{\varpi}(\varepsilon_i) z_i] \right|.\end{aligned}$$

where  $z_i := \sum_{(j,k,l)} \mathcal{X}_{i(j,k,l)} \mathcal{T}_{(j,k,l)}$ . For the first term, since  $|\ell'_1(x) - x| \lesssim x^2$ , we have

$$\begin{aligned}|\mathbb{E} [\ell'_{\varpi}(\varepsilon_i) z_i] - \mathbb{E} [\varepsilon_i z_i]| &\leq \varpi |\mathbb{E} [\{\ell'_1(\varepsilon_i/\varpi) - \varepsilon_i/\varpi\} z_i]| \\ &\lesssim \varpi^{-1} |\mathbb{E} [\varepsilon_i^2 z_i]| \lesssim \varpi^{-1} M K \sqrt{\frac{k}{k-1}}.\end{aligned}$$

For the second term, since  $|\ell'_\varpi(\varepsilon_i)| = |\varpi \ell'_1(\varepsilon_i/\varpi)| \leq \min\{c_1\varpi, |\varepsilon_i|\}$ , then for any  $q \geq 2$ ,

$$\begin{aligned} & \mathbb{E} |\ell'_\varpi(\varepsilon_i) z_i|^q \\ & \leq (c_1\varpi)^{q-2} \mathbb{E} |\varepsilon_i^2 z_i^q| \leq (c_1\varpi)^{q-2} \sqrt[k]{\mathbb{E} \left( \mathbb{E} (|\varepsilon_i|^2 | \mathcal{X}_i)^k \right) \left( \mathbb{E} |z_i^{\frac{qk}{k-1}}| \right)^{\frac{k-1}{k}}} \\ & \leq (c_1\varpi)^{q-2} M \left( \frac{K^2 q k}{k-1} \right)^{q/2} \leq q! M \left( e K c_1 \varpi \sqrt{\frac{2k}{k-1}} \right)^{q-2}. \end{aligned}$$

Therefore, by following the proof in (A.1)–(A.4), we obtain that

$$\mathbb{P} \left( \xi \leq C_5 \left( \frac{M df}{n} \right)^{\frac{1}{2}} (\sqrt{t} + t) \right) \geq 1 - 2 \exp(df(\log(13) - t)).$$

**Lemma 2.** Consider  $\{\eta_i\}_{i=1}^n$  are i.i.d. with  $\mathbb{E}[\eta_i^2] \leq M$  and  $\{X_i\}_{i=1}^n$  are  $n$  i.i.d. random  $d_1 \times d_2$  matrices whose entries  $X_{i(j,k)}$  are i.i.d. sub-gaussian random variables with  $\|X_{i(j,k)}\|_{\psi_2} = K$ . Denote  $A = \frac{1}{n} \sum_{i=1}^n \psi_\tau(\eta_i) X_i$  where  $\tau$  is given in Theorem 1. Then there exist positive constants  $C$  and  $c$  depending only on  $K$  such that

$$\begin{aligned} & \mathbb{P} \left( \sigma_{\max}^2(A) \leq \frac{\mathbb{E}[\psi_\tau(\eta_i)^2] + \tau^2 \sqrt{\frac{2t}{n}}}{n} \left( \sqrt{d_1} + C \sqrt{d_2} + \sqrt{2t} \right)^2 \right) \geq 1 - 2e^{-ct}, \\ & \mathbb{P} \left( \sigma_{\min}^2(A) \geq \frac{\mathbb{E}[\psi_\tau(\eta_i)^2] - \tau^2 \sqrt{\frac{2t}{n}}}{n} \left( \sqrt{d_1} - C \sqrt{d_2} - \sqrt{2t} \right)^2 \right) \geq 1 - 2e^{-ct}. \end{aligned}$$

*Proof.* This lemma is proved in a similar manner to the proof of Lemma 6 in Zhang et al. (2020). Since  $\|\frac{1}{n} \sum_{i=1}^n \psi_\tau(\eta_i) X_{i(j,k)}\|_{\psi_2} \leq K \sqrt{\sum_{i=1}^n \psi_\tau(\eta_i)^2 / n}$  for

given  $\{\psi_\tau(\eta_i)\}_{i=1}^n$ , by Theorem 5.39 in [Vershynin \(2012\)](#), we obtain that

$$\begin{aligned} \mathbb{P}\left(\sigma_{\max}^2(A) \geq \frac{\sum_{i=1}^n \psi_\tau(\eta_i)^2}{n^2} \left(\sqrt{d_1} + C\sqrt{d_2} + \sqrt{2t}\right)^2 \middle| \{\psi_\tau(\eta_i)\}_{i=1}^n\right) &\leq e^{-ct}, \\ \mathbb{P}\left(\sigma_{\min}^2(A) \leq \frac{\sum_{i=1}^n \psi_\tau(\eta_i)^2}{n^2} \left(\sqrt{d_1} - C\sqrt{d_2} - \sqrt{2t}\right)^2 \middle| \{\psi_\tau(\eta_i)\}_{i=1}^n\right) &\leq e^{-ct}. \end{aligned}$$

For  $\frac{1}{n} \sum_{i=1}^n \psi_\tau(\eta_i)^2$ , by Hoeffding's inequality, we can get that

$$\begin{aligned} \mathbb{P}\left(\frac{1}{n} \sum_{i=1}^n \psi_\tau(\eta_i)^2 - \mathbb{E}[\psi_\tau(\eta_i)^2] \geq \tau^2 \sqrt{\frac{2t}{n}}\right) &\leq e^{-t}, \\ \mathbb{P}\left(\frac{1}{n} \sum_{i=1}^n \psi_\tau(\eta_i)^2 - \mathbb{E}[\psi_\tau(\eta_i)^2] \leq -\tau^2 \sqrt{\frac{2t}{n}}\right) &\leq e^{-t}. \end{aligned}$$

Therefore,

$$\begin{aligned} &\mathbb{P}\left(\sigma_{\max}^2(A) \leq \frac{\mathbb{E}[\psi_\tau(\eta_i)^2] + \tau^2 \sqrt{\frac{2t}{n}}}{n} \left(\sqrt{d_1} + C\sqrt{d_2} + \sqrt{2t}\right)^2\right) \\ &\geq \mathbb{P}\left(\frac{1}{n} \sum_{i=1}^n \psi_\tau(\eta_i)^2 \leq \mathbb{E}[\psi_\tau(\eta_i)^2] + \tau^2 \sqrt{\frac{2t}{n}}\right) \\ &\quad \times \mathbb{P}\left(\sigma_{\max}^2(A) \leq \frac{\sum_{i=1}^n \psi_\tau(\eta_i)^2}{n^2} \left(\sqrt{d_1} + C\sqrt{d_2} + \sqrt{2t}\right)^2 \middle| \{\psi_\tau(\eta_i)\}_{i=1}^n\right) \\ &\geq 1 - 2e^{-ct}, \end{aligned}$$

$$\begin{aligned}
& \mathbb{P} \left( \sigma_{\min}^2(A) \geq \frac{\mathbb{E}[\psi_\tau(\eta_i)^2] - \tau^2 \sqrt{\frac{2t}{n}}}{n} \left( \sqrt{d_1} - C\sqrt{d_2} - \sqrt{2t} \right)^2 \right) \\
& \geq \mathbb{P} \left( \frac{1}{n} \sum_{i=1}^n \psi_\tau(\eta_i)^2 \geq \mathbb{E}[\psi_\tau(\eta_i)^2] - \tau^2 \sqrt{\frac{2t}{n}} \right) \\
& \quad \times \mathbb{P} \left( \sigma_{\min}^2(A) \geq \frac{\sum_{i=1}^n \psi_\tau(\eta_i)^2}{n^2} \left( \sqrt{d_1} - C\sqrt{d_2} - \sqrt{2t} \right)^2 \mid \{\psi_\tau(\eta_i)\}_{i=1}^n \right) \\
& \geq 1 - 2e^{-ct}.
\end{aligned}$$

□

**Lemma 3.** Consider  $\{X_i\}_{i=1}^n$  are  $n$  i.i.d. random  $d_1 \times d_2$  matrices whose entries are i.i.d. sub-gaussian random variables and  $\{y_i\}_{i=1}^n$  are from Eq. (1). Then there exists a constant  $C$  such that with probability at least  $1 - 2e^{-(d_1+d_2)(\log(7)-t)}$ ,

$$\left\| \frac{1}{n} \sum_{i=1}^n \psi_\tau(y_i) X_i - \mathbb{E}[y_i X_i] \right\|_{\text{op}} \leq C \left( \frac{df}{Mn} \right)^{\frac{1}{2}} \left( \sqrt{(d_1 + d_2)t/df} + (d_1 + d_2)t/df + 1 \right).$$

*Proof.* By the triangle inequality,

$$\begin{aligned}
& \left\| \frac{1}{n} \sum_{i=1}^n \psi_\tau(y_i) X_i - \mathbb{E}[y_i X_i] \right\|_{\text{op}} \\
& \leq \left\| \mathbb{E}[\psi_\tau(y_i) X_i] - \mathbb{E}[y_i X_i] \right\|_{\text{op}} + \left\| \frac{1}{n} \sum_{i=1}^n \psi_\tau(y_i) X_i - \mathbb{E}[\psi_\tau(y_i) X_i] \right\|_{\text{op}}.
\end{aligned}$$

Denote  $z_i := u^\top X_i v$  where  $u \in \mathbb{S}^{d_1-1}$  and  $v \in \mathbb{S}^{d_2-1}$ .  $\frac{1}{n} \sum_{i=1}^n \psi_\tau(y_i) u^\top X_i v = \frac{1}{n} \sum_{i=1}^n \psi_\tau(y_i) z_i$ . Since  $z_i$  is sub-Gaussian random variable with  $\|z_i\|_{\psi_2} = K$ , by using the similar treatment with (A.3), we obtain that for some constants

$C_1$  and  $C_2$  depending only on  $K, k$ , and  $c$ ,

$$\begin{aligned}
& \|\mathbb{E}[\psi_\tau(y_i)X_i] - \mathbb{E}[y_iX_i]\|_{\text{op}} \\
&= \sup_{u,v} |\mathbb{E}[\psi_\tau(y_i)z_i] - \mathbb{E}[y_iz_i]| \leq C_1 \left( M^{1/k} + c_1^2 \|\mathcal{A}^*\|_F^2 \right) / \tau \\
&\leq C_2 \left( M + c_1^2 \|\mathcal{A}^*\|_F^2 \right) \left( \frac{df}{Mn} \right)^{\frac{1}{2}}.
\end{aligned} \tag{B.1}$$

For the second term, according to (A.1) and (A.2), there exists an absolute constant  $C_3$  depending on  $K, k$  and  $c$  such that

$$\mathbb{P} \left( \left| \frac{1}{n} \sum_{i=1}^n \psi_\tau(y_i)z_i - \mathbb{E}[\psi_\tau(y_i)z_i] \right| \leq C_3 \sqrt{\frac{Mt}{n}} + C_3 \frac{\tau t}{n} \right) \geq 1 - 2e^{-t}.$$

Let  $\mathcal{N}_{\frac{1}{3}}^{d_1}$  and  $\mathcal{N}_{\frac{1}{3}}^{d_2}$  be  $\frac{1}{3}$ -nets of  $\mathbb{S}^{d_1-1}$  and  $\mathbb{S}^{d_2-1}$  respectively, where  $|\mathcal{N}_{\frac{1}{3}}^{d_1}| \leq 7^{d_1}$  and  $|\mathcal{N}_{\frac{1}{3}}^{d_2}| \leq 7^{d_2}$ . There exist  $u_1 \in \mathcal{N}_{\frac{1}{3}}^{d_1}$  and  $v_1 \in \mathcal{N}_{\frac{1}{3}}^{d_2}$  such that  $\|u - u_1\|_2 \leq 1/3$  and  $\|v - v_1\|_2 \leq 1/3$ . Thus, for any matrix  $A \in \mathbb{R}^{d_1 \times d_2}$ , we have

$$\begin{aligned}
u^\top Av &= u_1^\top Av_1 + (u - u_1)^\top Av_1 + u_1^\top A(v - v_1) + (u - u_1)^\top A(v - v_1) \\
&\leq \sup_{u \in \mathcal{N}_{\frac{1}{3}}^{d_1}, v \in \mathcal{N}_{\frac{1}{3}}^{d_2}} u^\top Av + \left( \frac{1}{3} + \frac{1}{3} + \frac{1}{9} \right) \sup_{u \in \mathbb{S}^{d_1-1}, v \in \mathbb{S}^{d_2-1}} u^\top Av.
\end{aligned}$$

Thus,  $\|A\|_{\text{op}} \leq \frac{9}{2} \sup_{u \in \mathcal{N}_{\frac{1}{3}}^{d_1}, v \in \mathcal{N}_{\frac{1}{3}}^{d_2}} u^\top Av$ . Therefore, the following inequality holds:

$$\left\| \frac{1}{n} \sum_{i=1}^n \psi_\tau(y_i)X_i - \mathbb{E}[\psi_\tau(y_i)X_i] \right\|_{\text{op}} \leq \frac{9}{2} \max_{\substack{u \in \mathcal{N}_{\frac{1}{3}}^{d_1} \\ v \in \mathcal{N}_{\frac{1}{3}}^{d_2}}} \left| \frac{1}{n} \sum_{i=1}^n \psi_\tau(y_i)z_i - \mathbb{E}[\psi_\tau(y_i)z_i] \right|.$$

By using the union bound for all  $u \in \mathcal{N}_{\frac{1}{3}}^{d_1}$  and  $v \in \mathcal{N}_{\frac{1}{3}}^{d_2}$  and (A.5), we have with probability at least  $1 - 2e^{(d_1+d_2)(\log(7)-t)}$ ,

$$\begin{aligned}
& \left\| \frac{1}{n} \sum_{i=1}^n \psi_\tau(y_i) X_i - \mathbb{E} [\psi_\tau(y_i) X_i] \right\|_{\text{op}} \\
& \leq C_4 \sqrt{\frac{M(d_1 + d_2)t}{n}} + C_4 \frac{\tau(d_1 + d_2)t}{n} \\
& \leq C_5 M^{\frac{1}{2}} \left( \frac{df}{n} \right)^{\frac{1}{2}} \left( \sqrt{(d_1 + d_2)t/df} + (d_1 + d_2)t/df \right). \tag{B.2}
\end{aligned}$$

Therefore, the conclusion holds by combining (B.1) with (B.2).  $\square$

## References

- Boucheron, S., Lugosi, G., Massart, P., 2013. Concentration inequalities: A nonasymptotic theory of independence. Oxford University Press. doi:[10.1093/acprof:oso/9780199535255.001.0001](https://doi.org/10.1093/acprof:oso/9780199535255.001.0001).
- Cai, T.T., Zhang, A., 2018. Rate-optimal perturbation bounds for singular subspaces with applications to high-dimensional statistics. The Annals of Statistics 46, 60–89. doi:[10.1214/17-AOS1541](https://doi.org/10.1214/17-AOS1541).
- De Lathauwer, L., De Moor, B., Vandewalle, J., 2000. A multilinear singular value decomposition. SIAM Journal on Matrix Analysis and Applications 21, 1253–1278. doi:[10.1137/S0895479896305696](https://doi.org/10.1137/S0895479896305696).
- Du, S., Li, T., Yang, Y., Horng, S.J., 2021. Deep air quality forecasting using hybrid deep learning framework. IEEE Transactions on Knowledge and Data Engineering 33, 2412–2424. doi:[10.1109/TKDE.2019.2954510](https://doi.org/10.1109/TKDE.2019.2954510).
- Fan, J., Gu, Y., Zhou, W.X., 2024. How do noise tails impact on deep ReLU networks? The Annals of Statistics 52, 1845–1871. doi:[10.1214/24-AOS2428](https://doi.org/10.1214/24-AOS2428).



- Fan, J., Ke, Y., Sun, Q., Zhou, W.X., 2019. FarmTest: Factor-adjusted robust multiple testing with approximate false discovery control. *Journal of the American Statistical Association* 114, 1880–1893. doi:[10.1080/01621459.2018.1527700](https://doi.org/10.1080/01621459.2018.1527700).
- Fan, J., Li, Q., Wang, Y., 2016. Estimation of high dimensional mean regression in the absence of symmetry and light tail assumptions. *Journal of the Royal Statistical Society Series B: Statistical Methodology* 79, 247–265. doi:[10.1111/rssb.12166](https://doi.org/10.1111/rssb.12166).
- Fan, J., Wang, W., Zhu, Z., 2021. A shrinkage principle for heavy-tailed data: High-dimensional robust low-rank matrix recovery. *The Annals of Statistics* 49, 1239–1266. doi:[10.1214/20-AOS1980](https://doi.org/10.1214/20-AOS1980).
- Han, R., Willett, R., Zhang, A.R., 2022. An optimal statistical and computational framework for generalized tensor estimation. *The Annals of Statistics* 50, 1–29. doi:[10.1214/21-AOS2061](https://doi.org/10.1214/21-AOS2061).
- Huber, P.J., 1964. Robust estimation of a location parameter. *The Annals of Mathematical Statistics* 35, 73–101. doi:[10.1214/aoms/1177703732](https://doi.org/10.1214/aoms/1177703732).
- Kong, D., An, B., Zhang, J., Zhu, H., 2020. L2RM: Low-rank linear regression models for high-dimensional matrix responses. *Journal of the American Statistical Association* 115, 403–424. doi:[10.1080/01621459.2018.1555092](https://doi.org/10.1080/01621459.2018.1555092).
- Latała, R., 2005. Some estimates of norms of random matrices. *Proceedings of the American Mathematical Society* 133, 1273–1282. doi:[10.1090/s0002-9939-04-07800-1](https://doi.org/10.1090/s0002-9939-04-07800-1).
- Liu, L., Zhang, D., 2025. A Bernstein-type inequality for high dimensional linear processes with applications to robust estimation of time series regressions. *Statistica Sinica* 35, 151–170. doi:[10.5705/ss.202022.0249](https://doi.org/10.5705/ss.202022.0249).
- Lu, W., Zhu, Z., Lian, H., 2020. High-dimensional quantile tensor regression. *Journal of Machine Learning Research* 21, 1–31. URL: <http://jmlr.org/papers/v21/20-383.html>.
- Luo, B., Gao, X., 2022. High-dimensional robust approximated M-estimators for mean regression with asymmetric data. *Journal of Multivariate Analysis* 192, 105080. doi:[10.1016/j.jmva.2022.105080](https://doi.org/10.1016/j.jmva.2022.105080).

- Man, R., Tan, K.M., Wang, Z., Zhou, W.X., 2024. Retire: Robust expectile regression in high dimensions. *Journal of Econometrics* 239, 105459. doi:[10.1016/j.jeconom.2023.04.004](https://doi.org/10.1016/j.jeconom.2023.04.004).
- Negahban, S., Wainwright, M.J., 2011. Estimation of (near) low-rank matrices with noise and high-dimensional scaling. *The Annals of Statistics* 39, 1069–1097. doi:[10.1214/10-AOS850](https://doi.org/10.1214/10-AOS850).
- Recht, B., Fazel, M., Parrilo, P.A., 2010. Guaranteed minimum-rank solutions of linear matrix equations via nuclear norm minimization. *SIAM Review* 52, 471–501. doi:[10.1137/070697835](https://doi.org/10.1137/070697835).
- Shen, Y., Li, J., Cai, J.F., Xia, D., 2025. Computationally efficient and statistically optimal robust high-dimensional linear regression. *The Annals of Statistics* 53, 374–399. doi:[10.1214/24-AOS2473](https://doi.org/10.1214/24-AOS2473).
- Sun, Q., Zhou, W.X., Fan, J., 2020. Adaptive Huber regression. *Journal of the American Statistical Association* 115, 254–265. doi:[10.1080/01621459.2018.1543124](https://doi.org/10.1080/01621459.2018.1543124).
- Vershynin, R., 2012. Introduction to the non-asymptotic analysis of random matrices. Cambridge University Press, Cambridge, UK. chapter 5. p. 210–268.
- Wakin, M.B., Laska, J.N., Duarte, M.F., Baron, D., Sarvotham, S., Takhar, D., Kelly, K.F., Baraniuk, R.G., 2006. An architecture for compressive imaging, in: 2006 International Conference on Image Processing, pp. 1273–1276. doi:[10.1109/ICIP.2006.312577](https://doi.org/10.1109/ICIP.2006.312577).
- Wang, D., Tsay, R.S., 2023. Rate-optimal robust estimation of high-dimensional vector autoregressive models. *The Annals of Statistics* 51, 846–877. doi:[10.1214/23-AOS2278](https://doi.org/10.1214/23-AOS2278).
- Wang, L., Zheng, C., Zhou, W., Zhou, W.X., 2021. A new principle for tuning-free Huber regression. *Statistica Sinica* 31, 2153–2177. doi:[10.5705/ss.202019.0045](https://doi.org/10.5705/ss.202019.0045).
- Zhang, A.R., Luo, Y., Raskutti, G., Yuan, M., 2020. ISLET: Fast and optimal low-rank tensor regression via importance sketching. *SIAM Journal on Mathematics of Data Science* 2, 444–479. doi:[10.1137/19M126476X](https://doi.org/10.1137/19M126476X).

- Zhou, W.X., Bose, K., Fan, J., Liu, H., 2018. A new perspective on robust  $M$ -estimation: Finite sample theory and applications to dependence-adjusted multiple testing. The Annals of Statistics 46, 1904–1931. doi:[10.1214/17-AOS1606](https://doi.org/10.1214/17-AOS1606).
- Zhu, Z., Zhou, W., 2021. Taming heavy-tailed features by shrinkage, in: Banerjee, A., Fukumizu, K. (Eds.), Proceedings of The 24th International Conference on Artificial Intelligence and Statistics, PMLR. pp. 3268–3276. URL: <https://proceedings.mlr.press/v130/zhu21c.html>.